Doing More with Ambient Light: Harvesting Indoor Energy and Data Using Emerging Solar Cells

Johann Bouclé, Daniel Ribeiro dos Santos, Anne Julien-Vergonjanne

solar

MDPI

Review

Doing More with Ambient Light: Harvesting Indoor Energy and Data Using Emerging Solar Cells

Johann Bouclé [1,2,*], Daniel Ribeiro Dos Santos [1,2] and Anne Julien-Vergonjanne [1,2]

[1] XLIM, UMR 7252, University of Limoges, F-87000 Limoges, France
[2] CNRS, XLIM, UMR 7252, F-87000 Limoges, France
* Correspondence: johann.boucle@unilim.fr; Tel.: +33-5-87-50-67-62

Abstract: On one side, the capacity of the world's photovoltaic (PV) systems is experiencing unprecedented growth; on the other side, the number of connected devices is rapidly increasing due to the development of advanced communication technologies. These fields are not completely independent, and recent studies show that indoor energy harvesting is a great candidate for answering the energy challenges of future generations of telecommunications, namely 5G and 6G, ideal for internet-of-things (IoT) scenarios, i.e., smart homes, smart cities, and smart factories. The emerging PV technologies have shown amazing capabilities for indoor energy harvesting, displaying high power conversion efficiency, good flexibility, and champion-specific powers. Recently, the excellent dynamic performance of PV devices enabled them to be used as data receivers in optical wireless communication (OWC) scenarios, calling forth an innovative system able to simultaneously harvest energy and receive communication data with a single PV device. This article reviews the recent literature devoted to the exploitation of photovoltaic technologies for simultaneous indoor energy harvesting and OWC data reception. This contribution highlights the strong potential of the approach toward the next generation of Green IoT systems and the current challenges that need to be addressed with regard to the physics of solar cells, from laboratory to large-scale applications.

Keywords: photovoltaics; solar cells; indoor photovoltaics; IoT; visible light communications (VLC); optical wireless communications (OWC); energy harvesting

Citation: Bouclé, J.; Ribeiro Dos Santos, D.; Julien-Vergonjanne, A. Doing More with Ambient Light: Harvesting Indoor Energy and Data Using Emerging Solar Cells. *Solar* **2023**, *3*, 161–183. https://doi.org/10.3390/solar3010011

Academic Editors: Jürgen Heinz Werner and Sadia Ameen

Received: 3 January 2023
Revised: 15 March 2023
Accepted: 16 March 2023
Published: 20 March 2023

1. Introduction

Solar resources appear to be a highly strategic alternative to fossil fuels in the context of the unprecedented climatic and energetic challenges faced by our modern societies. In a world where human activity is becoming significantly challenged by Earth's physical limits, reducing our carbon dioxide emissions and environmental footprint is crucial. In this picture, any applied technology has to demonstrate highly efficient systems and must comply with a broad set of specifications to minimize its environmental impact (use of abundant raw materials, greenhouse gas emission, virtuous lifecycle), energetic consumption, and cost, while maximizing its lifetime, robustness, and recycling ability.

Regarding energy supply and world electricity production, solar energy conversion, especially solar photovoltaics (PV), has demonstrated a constant rise in the last decades, achieving a global capacity of ~160 GW in 2021. Corresponding to an unprecedented growth rate of 17%, this rise accounts for 60% of all renewable technologies capacity growth, despite growing manufacturing costs observed over the last few years [1]. Recent reports highlight the true potential of solar PV for large-scale electricity generation in a zero net emission scenario, allowed by expected efficiency improvements (at the sub-cell and module levels), but also through scaling laws of industrial processes, as well as softer regulations and incitation policies [2]. Moreover, economic and environmental indicators of solar PV show a regular decrease in both the levelized cost of energy (LCOE) and the energy payback time (EPBT) [3,4], which further pushes investments in the technology.

Indeed, the current LCOE of utility-scale solar PV is already below 0.03 USD/kWh in some regions of the world, and they should keep showing a global decreasing trend by the end of the decade. At the same time, the cost of fossil fuels and nuclear electricity production has increased in recent years—with an increasing impact of CO_2 emission contributions to the final price—and the trend is not expected to reverse in the near future [4]. While silicon technologies still largely dominate the market of grid-connected or off-grid solar PV, emerging photovoltaic technologies mainly based on thin film architectures have been developed and explored from the fundamental point of view and also at industrial or pre-industrial levels in some cases. Thin film PV technologies include second-generation devices based on copper–indium–gallium–selenide (CIGS), cadmium telluride (CdTe), amorphous silicon (a-Si), and high-efficiency gallium-arsenide (GaAs) cells, as well as emerging PV technologies such as quantum-dot photovoltaics (QDPV), dye-sensitized solar cells (DSSC), organic photovoltaics (OPV), and perovskite solar cells (PSC) [5]. Low-cost technologies (mainly QDPV, DSSC, OPV, and perovskite) are attracting the specific attention of researchers and industrial actors worldwide due to the possibility of exploiting fewer raw materials, as well as printing technologies in soft environmental conditions (low temperatures, ambient atmosphere, etc.) over a large area [6–8]. Additionally, despite strong challenges associated with device lifetime and durability under outdoor operating conditions, several of these technologies have shown drastic efficiency improvements under standard test conditions, or STC, (100 $mW \cdot cm^{-2}$, AM1.5G solar spectrum, 25 °C) over the last years, leading to efficiencies that compete with conventional thin film technologies (in some cases overperforming conventional thin film technologies, see Table 1). For example, power conversion efficiencies (PCE) of OPV have shown a drastic increase between 2018 and 2022, from 13% to over 18% under STC, due to unprecedented advances in organic semiconducting materials and energy loss minimization [9], while perovskite devices nearly reached PCE of 26% using bandgap and interfacial engineering, as well as defect management [10]. More recently, perovskite heterojunctions also passed damp heat testing (85 °C and 85% relative humidity), a key industry standard for commercial applications [11].

Table 1. Reported maximum power conversion efficiencies of the main PV technologies under solar illumination (AM1.5G solar spectrum) and under typical indoor illumination conditions.

PV Technology	1 Sun Efficiency (STC) *	Indoor Efficiency **	Illumination	Reference
Monocrystalline Si	26.1%	~6%	1000 Lux LED	[12]
Polycrystalline Si	23.3%	~4%	1000 Lux LED	[12]
CIGS	23.4%	9.4%	1000 Lux FL	[13]
Amorphous Si	14.0%	19–21%	1000 Lux LED	[14]
GaAs	29.1%	19%	580 Lux LED	[14]
Dye-sensitized	13.0%	31.8%	1000 Lux FL	[15]
OPV	18.2%	31.0%	1650 Lux LED	[16]
Perovskites	25.7%	40.2%	1000 Lux FL	[17]
Quantum dot solar cells	18.1%	19.5%	2000 Lux FL	[18]

* STC = standard test conditions. STC data are extracted from NREL's best research-cell efficiencies, available at https://www.nrel.gov/pv/cell-efficiency.html (accessed on 15 March 2023). ** Indoor efficiencies are taken from independent reports cited in the reference column. The illumination level and technology are indicated: fluorescent lamp (FL); light-emitting diodes (LED).

Such levels of performance give confidence that emerging PV can be relevant alternatives to inorganic technologies in some outdoor scenarios. However, stability and costs remain crucial to competing with classical silicon-based devices, despite intrinsic low-cost processing technologies. Recent cost analyses, for example, demonstrated that classical OPV modules based on Indium-free electrodes and non-fullerene organic materials for active layers would still see their cost mainly dominated by active layer materials (to more than 80%) for small-scale production systems, while drastic cost reduction of raw materials could be achieved for large-scale facilities (production capacity > 1 MW) [19]. Moreover, a detailed analysis of operating costs of OPV technology in China revealed LCOE ranging from 0.2 RMB/kWh for OPV mod-

ules with 20% efficiency and a 20-year lifetime up to 1.8 RMB/kWh for a 5% efficient module with a 6-year lifetime, showing the main limitations to industrial upscaling of OPV. Regarding perovskite modules, although research assumptions can vary widely and lead to some large estimations, recent studies show that the LCOE can reach 0.05 to 0.10 USD/kWh for residential use, considering high-efficiency modules (>16%) with a long lifetime (>20 years) [20,21]. Tandem devices (either perovskite/perovskite or silicon/perovskite modules) have also been evaluated from the economic point of view, considering the high efficiencies recently achieved for silicon/perovskite tandems (>32%) [22]. Low LCOE (below 0.1 USD/kWh) could be achieved in all cases, including tandem and single junction devices, as long as decent lifetime and efficiencies can be achieved, which remains a large challenge in the field (as well as lead reduction). In parallel, the environmental impact and energy costs of PV technologies should be considered for any commercial applications. A recent report emphasizes the viability of perovskite technologies for a low environmental footprint as long as material recycling is involved [23]. Compared to classical silicon-based modules, perovskite technology shows a very promising environmental footprint, with an EPBT as low as 0.09 years and a greenhouse gas (GHG) emission factor of 13.4 g CO_2 equivalent per kWh, as compared to 1.3–2.4 years EPBT and GHG factor of 22.1–38.1 g CO_2 for the market leading silicon [24]. Transparent OPV modules also demonstrate a very low energy footprint with EPBT as low as 113 days (0.3 years), which can be reduced to 0.14 years for building-integrated applications [25]. In all cases, these levels of environmental and energetic performance are still strongly dependent on device efficiencies and lifetimes.

Such levels of performance give confidence that emerging PV can be relevant alternatives to inorganic technologies in some outdoor scenarios, but their true potential must be considered for indoor applications, as mild ambient conditions (illumination levels 1000 to 10,000 times lower than outdoor; reduced operation temperature) make them more robust and stable. This trend is clearly observed in the recent literature on indoor photovoltaics [14,26,27], which shows a drastic increase in the last 10 years (see Figure 1a). The strong potential of emerging PV for indoor photovoltaics is also justified by theoretical considerations about the maximum achievable efficiencies under artificial illumination [27–30]. Indeed, unlike the very broad emission coming from the Sun (from 350 up to 1800 nm), artificial illumination relies on light sources presenting narrow spectral coverage (over 400–700 nm for most white light-emitting diodes and compact fluorescent light bulbs and up to only 900–1000 nm for incandescent light sources, see Figure 1b), which drastically modify the absorber requirements and, consequently, the maximal achievable power conversion efficiency from the classical Shockley–Quiesser (SQ) approach.

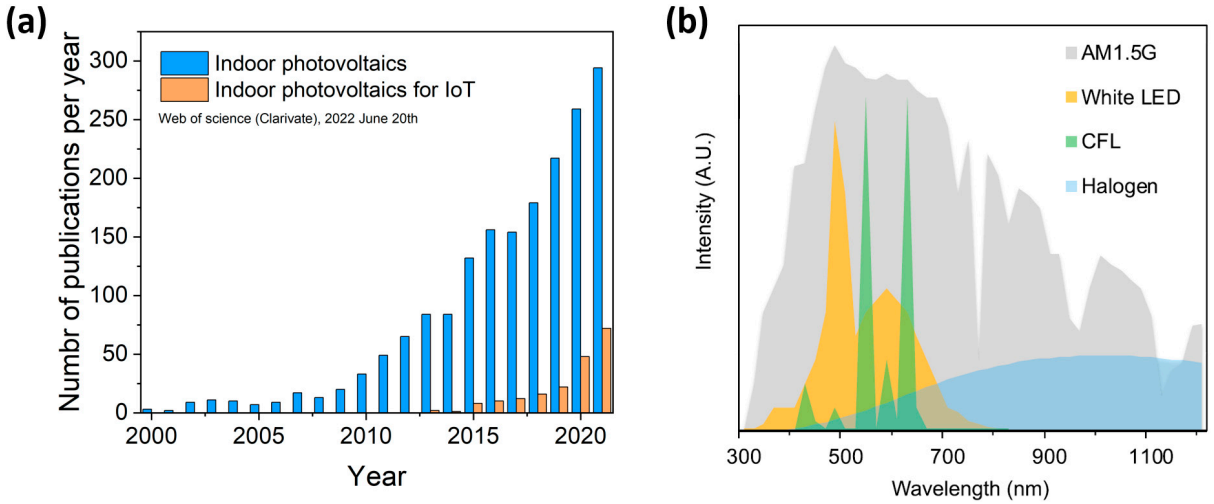

Figure 1. (**a**) Recent bibliography on indoor photovoltaics and on indoor photovoltaics claiming applications for IoT. Data extracted from Web of Science (Clarivate) in July 2022; (**b**) Normalized irradiance of light sources including standard solar spectrum (AM1.5G), white LED, compact fluorescent lamps (CFL), and halogen source. Reprinted from reference [31], with permission from Elsevier.

Ideal bandgaps of 1.4–1.5 eV are usually considered under the AM1.5G solar spectrum; larger bandgaps of 1.9–2.0 eV are expected to perform better under indoor conditions, associated with SQ efficiency limits up to 57% [30,32]. In this picture, emerging PV technologies based on larger bandgap materials that can easily be tuned by soft chemistry appear highly relevant as they limit thermal losses associated with conventional low-bandgap PV absorbers while allowing high open-circuit voltages. To illustrate these features, the current indoor power conversion efficiencies of the main PV technologies are compared in Table 1: emerging thin film PV technologies are clearly ahead of classical PV materials. PCE of 32% [15], 31% [16], and up to 40.1% [17] under artificial illumination are evidenced for DSSC, OPV, and perovskite devices, respectively. Many recent progress reports show the same trends for these technologies [33–35]. Such levels of performance give these technologies a strong relevance for energy harvesting applications in many scenarios.

This aspect is crucial in the context of the internet-of-things (IoT) ecosystem, which will face massive growth in the deployment of small sensors, actuators, and tools, allowing remote data collection and wireless communication in specific environments, from smart homes to smart cities and smart factories (Industry 4.0) [36]. From the energetic point of view, considering that most of these devices are employed in indoor scenarios, ambient energy harvesting is particularly relevant to demonstrate truly eco-energetic and sustainable IoT systems [37–39]. Considering record efficiencies under low-lighting conditions, the tuneability, low-cost processing, and ease of integration provided by flexible plastic substrates, emerging solution-processed PV technologies are considered particularly relevant to address these energy challenges [37–40]. Again, the recent bibliography points out a clear increase in the interest of emerging PV researchers in IoT applications, as seen in Figure 1a. The power density generated under conventional indoor illumination by state-of-the-art perovskite or organic PV devices is now above 150 $\mu W \cdot cm^{-2}$ [16,17], which enables enough power supply for a broad range of IoT nodes (smoke detectors, wall clocks, autonomous sensors, etc.) [31,38]. Finally, another crucial aspect of these technologies for IoT applications is their very high specific power (up to 30 $W \cdot g^{-1}$ have been reached for perovskite solar cells on polyethylene terephthalate foils [41], where state-of-the-art ultralight weight GaAs array shows around 5 $W \cdot g^{-1}$ [42]). This ease of integration is particularly crucial for autonomous IoT systems, as well as for powering wearable electronic devices [43,44]. Some recent reviews in the literature clearly emphasize the true potential of emerging PV technologies for IoT applications, including DSSC [45,46], OPV [31,47–49], and halide perovskites [50–53], by focusing on materials development, as well as interface and architecture engineering. Their great indoor lighting conversion performance and easy integration allowed their employment at autonomous ultra-low powered (ULP) radiofrequency (RF) devices for wireless sensing, a key factor for modern IoT [54]. However, RF technology currently faces multiple problems, such as saturation of its frequency spectrum and lack of physical security [55], issues that are limiting modern communication capabilities. To overcome saturation, a solution envisaged in future 6G networks is the use of new frequency bands, including optical bands. Thus, optical wireless communications (OWC) have many potentialities. Since optical signals are confined indoors, physical attacks on the signal are more difficult, so security is improved. Additionally, recent research has shown the interesting potential of PV devices acting as OWC receivers, allowing data reception and energy harvesting simultaneously. In the next sections of this article, we will focus on the aforementioned application of PV technologies in OWC scenarios, pointing out the main challenges in terms of device physics and the trade-off between energy harvesting and data reception capability.

2. Pushing PV Technologies Forward: Receiving Optical Data Using Solar Cells in the Context of IoT and Optical Wireless Communication

2.1. First Proof of Concept

The promising features of emerging solution-processed PV technologies to power indoor IoT devices were recently further extended to more exciting functionalities. Among new

usages or evolutions of solar cells (recently referred to in the field of *photovoltatronics* [56]), their use as optical data receivers in the context of visible light communications (VLC) was recently proposed. Indeed, IoT devices rely on wireless communication technologies for their interconnections. While radiofrequency-based technologies can address these challenges over moderate to long distances in the context of 5G and 6G [57], OWC show significant advantages related to the spatial confinement of optical waves, license-free deployment, and insensitivity to interferences while also being well-suited for a large panel of data rates from kbit/s to Gbit/s [58,59]. OWC are found to be particularly well suited for indoor scenarios over short distances and in specific environments where people's safety and data security are required. Today, research in the field of OWC in the visible (i.e., VLC in the 380–780 nm range) is rapidly increasing due to the penetration of LED lighting, which is compatible with high modulation speed [60].

In the context of PV cells as OWC receivers, the first proof of concept was proposed by Kim et al. using a typical 729 mm^2 Si solar panel to harvest solar energy and receive a VLC signal simultaneously. By analyzing the current-voltage or I(V) characteristics of the device for a given irradiance, the optimal load for maximum output power of the solar panel could be obtained, which was then placed under solar irradiation and under modulated light simultaneously [61]. Analyzing the output voltage of the receiver, the direct current (DC), which comes from the constant solar illumination, and alternating current (AC) (please note that DC and AC stand for current, but in the communication field it is also used to describe a direct/constant parameter—such as constant illumination or voltage offset—and a non-DC, not necessarily a sinusoid, respectively), which is due to the modulated light, could be recovered, giving at that time the first proof of concept of using a single photosensitive device for both purposes.

In 2014–2015, Haas's group went even further as they harvested energy and received data from the same source using a PV device, proposing a novel front-end circuit to improve both performances simultaneously [62,63]. The typical transmission/reception system is depicted in Figure 2, as well as the proposed equivalent electrical circuit of the photovoltaic receiver for the detection of both the DC (bias light for energy generation) and AC components (modulated amplitude for data transmission). The receiver circuit is built using adapted inductance and capacitance, which enables the direct separation of DC and AC branches. In this case, the conventional diode used in first-level equivalent circuits for the modeling of single junction solar cells is replaced by its small-signal equivalent resistor r, adding a junction capacitance C in parallel with the shunt resistance R_{SH}. The small-signal model is mainly used for communication purposes and describes the performance of the diode when influenced by a signal with small amplitude, analyzing only the AC condition of the system. The capacitor C_0 would not cause a change in the current flow direction since the DC current component is still greater than the AC one. Typical signals obtained using such simple receiver circuit are reported elsewhere to illustrate the concept [63,64]. The authors were able to use commercial solar panels (polycrystalline silicon modules, 432 cm^2, 5 Wp) to receive data and harvest energy simultaneously [62].

Using a direct line-of-sight (LOS) configuration with a transmitter (LED)/receiver distance of a few tens of centimeters, the authors demonstrated a bit error rate (BER) below 2×10^{-3} for a 1 Mbit/s on-off keying (OOK) modulated signal sent upon an irradiance of 3.5×10^{-4} $W{\cdot}cm^{-2}$ (equivalent to a low level of indoor illumination). More advanced modulation schemes based on the orthogonal frequency division multiplexing (OFDM) technique further pushed the data rate up to 7 Mbit/s. It is worth noting that the 3 dB bandwidth of the solar panel used was measured at 350 kHz in this case. In a second case study, the authors were able to push the performance up to 11.8 Mbit/s while exploring the main operating parameters (load resistances R_L and R_C, capacity C_0 and inductance L_0, see Figure 3 as an example) [63].

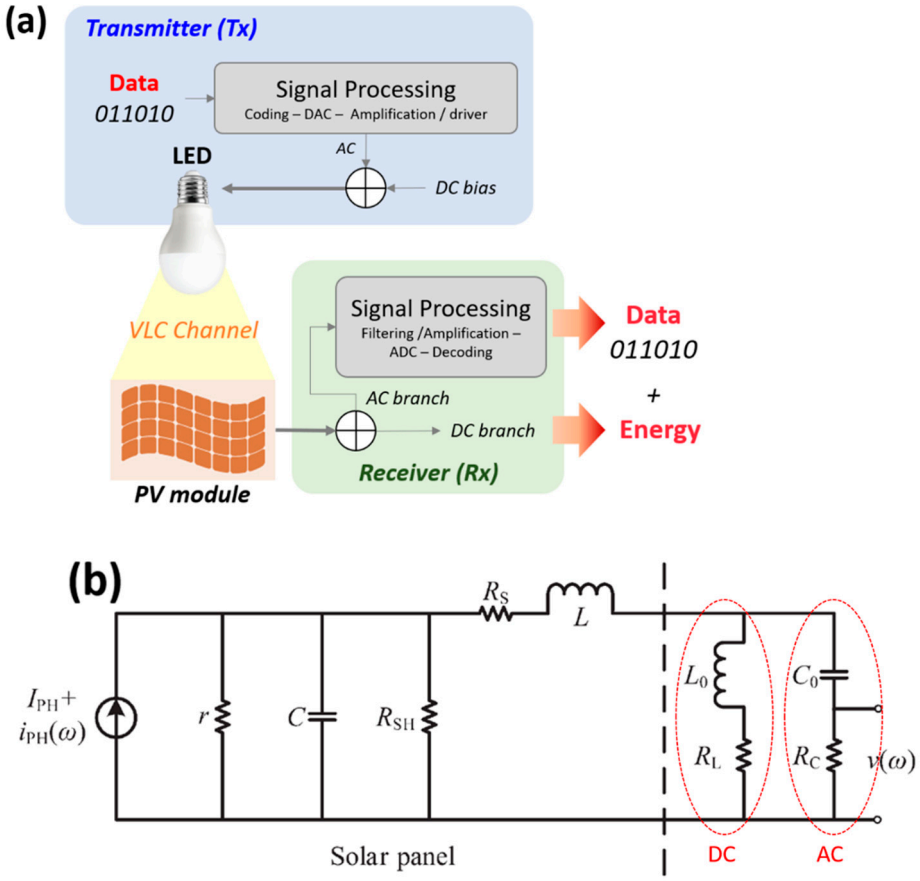

Figure 2. (**a**) Schematic representation of a typical VLC chain illustrating the dual operation of a PV module used as a receiver for simultaneously harvesting energy and optical data from modulated light; (**b**) Equivalent electrical circuit of a solar panel working in dynamic regime and connected to a receiver circuit enabling the reception of both electrical DC and AC components. Modified with permission from reference [63].

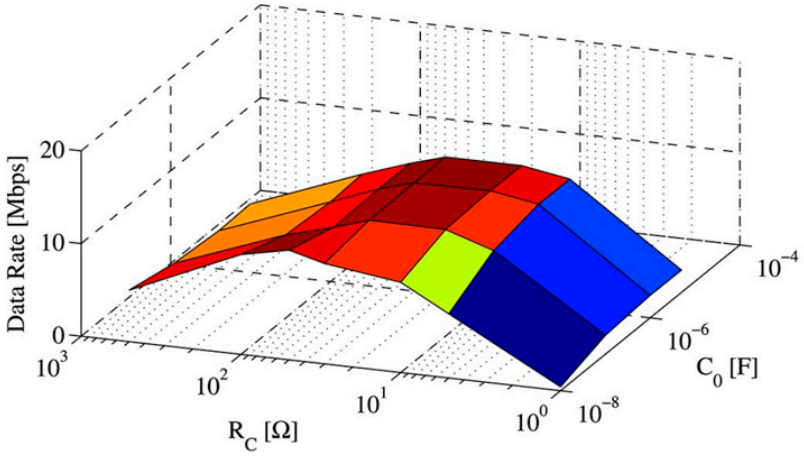

Figure 3. Maximum experimentally achieved data rate as a function of R_C and C_0, in an OFDM scenario targeting a BER $< 2 \times 10^{-3}$. Reproduced with permission from reference [63].

The first-level estimation of equivalent electrical circuit components enabled them to validate the small-signal linear model used to predict the solar panel frequency response. More importantly, these pioneered works demonstrated the feasibility of simultaneously harvesting energy and data from the solar panel. Received power of approximately 30 mW (equivalent to 165 $\mu W \cdot cm^{-2}$ power density) was harvested at the operation point that

provides the maximum data rate, considering a received irradiance swinging between 3.3 and 4 $\times$ 10^{-3} W·cm^{-2}.

A main advantage of the concept lies in the fact that solar panels are passive devices that do not require an additional power supply to convert the light AC component into an electrical signal, unlike conventional VLC receivers (photodiodes or photomultipliers), which require a trans-impedance amplifier [65]. Using solar cells instead of conventional photodetectors brings some specific features later discussed by many groups, such as limited rise and fall times but larger intrinsic output voltages. The impact of a large active area associated with solar panels versus a photodiode is also crucial for noise and gain management [66].

These reports opened the way to relevant innovations on the use of solar cells in the field of VLC applied to IoT, but they also brought many questions regarding the dynamic behavior of photovoltaic devices and modules and the necessary trade-off with their classical steady-state operation. Indeed, solar panels deliver their maximum power under specific load resistance. This maximum power point (MPP) is tracked in conventional PV installations, but it does not necessarily allow the best dynamics under modulated light, knowing that conventional photoreceivers (PIN photodiodes especially) need to be reverse-biased for maximal dynamics and linearity. We note that the concept of using a solar panel to simultaneously harvest energy and data led to the related SLIPT concept, which was proposed in 2018 by the wireless communications community as Simultaneous Lightwave Information and Power Transfer [67–70], and recently extended to IoT applications [71,72].

In the next section of this contribution, we review the recent developments made on the use of PV cells as receivers for simultaneously harvesting energy and data—i.e., in the context of SLIPT—with specific attention paid to the PV device itself and the associated physics. We will first describe works reported using conventional PV technologies (silicon-based, thin films) before focusing on emerging PV devices (OPV and perovskites) which have also been explored in this context. We will finally try to emphasize the main questions that should be tackled in terms of emerging PV architecture in order to address the main challenges of this rising field of applications, which has to merge the constraints of indoor operation at low illumination levels, and the constraints of quality of service (QoS) in terms of communication scenario. We will also discuss the difficulty of predicting the energy harvesting and data reception performance of solar modules in non-ideal scenarios (non-LOS) where complex environments and usages are involved, as required by the next generation of autonomous IoT nodes.

2.2. Harvesting Energy and Data Using Silicon-Based and Thin Films PV Technologies

Soon after the first proofs-of-concept previously described, several reports were published that illustrate various performances of simple VLC LOS scenarios using commercial and small-area solar panels based on silicon [73], some of them focusing only on the communication aspect, and others on the dual functionality. Attempts by Malik et al. focused on the receiver circuit in order to address the intrinsic distortions arising from the silicon-based solar panel [74]. The latter can be seen as a low-pass filter, which induces a limited response time through *RC* limitations, where *R* and *C* are effective high frequency resistance and capacitance whose physical origin remains under discussion, depending on the PV technology considered (as we will point out later on). This capacitive limitation deforms the electrical signal received at the device, considering that the incident light is modulated in amplitude, giving rise to a square signal, then limiting the communication performance of the system. Therefore, Malik et al. demonstrated a self-powered active receiver based on a signal conditioning unit, leading to error-free reception up to 8 kbit/s over 50 cm (OOK modulation) [74]. This work was followed in 2016 by a Yonsei University report in South Korea, which describes a receiver circuit able to apply a reverse bias at the solar panel (a small monocrystalline Si module in this case) in order to improve both the responsivity and response time of the device by benefiting from an increased carrier drift velocity [75], extending then the bandwidth of the PV device. By using the harvested en-

ergy of the DC branch to drive their dedicated reception circuit, they were able to improve the transmission performance up to 17 Mbit/s (BER of 10^{-3} over 10 cm) using discrete multitone (DMT) modulation. Using a DC-DC power converter, they were able to change the voltage of the solar cell, still harvesting energy while operating in the photodetection region, a technique that was further improved in 2021 [76].

Other classical strategies used in wireless communication technologies have also been applied to VLC systems based on solar cell receivers, such as using pre-distortion coding signals to mitigate the slow dynamic of solar panels [77,78], which brought faster data rates. Interestingly, the impact of additional parallel resistance in the equivalent electrical circuit before the detection of the solar panel output signal through the high impedance of an oscilloscope was shown to impact the device bandwidth and responsivity [78]. It is also worth mentioning more recent work devoted to increasing the data rate of silicon-based PV receivers using equalization as well as more complex modulation schemes (direct current optical DCO-OFDM or pulse amplitude modulation discrete multitone PAM-DMT) such as in [79], leading to data rates up to 74 Mbit/s (3.3 $\times$ 10^{-3} BER over 2 m).

Coming back to the solar panel receivers, in 2016, a joint team between CEA/LETI and SunPartner Technologies investigated the frequency response of thin film PV modules (CIGS from Disasolar and semi-transparent a-Si from SunPartner Technologies) as a function of illumination conditions between 200 and 300,000 Lux provided by an LED [80]. A drastic reduction in DCO-OFDM signal-to-noise ratio (SNR) is evidenced when ambient light noise is rising, especially for the CIGS module, which shows saturation effects (see Figure 4).

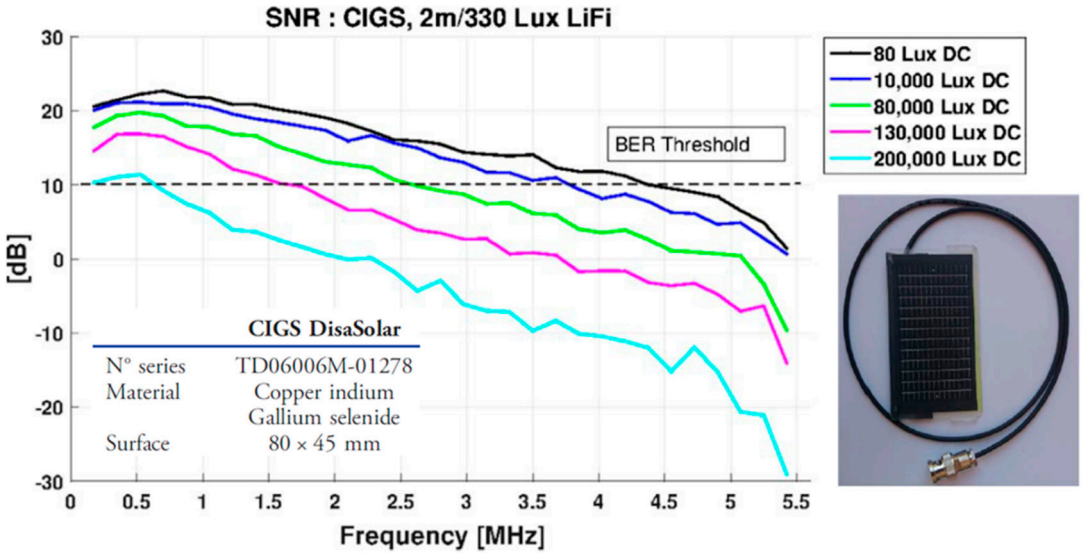

Figure 4. SNR of a DisasSolar CIGS module (illustrated in the picture on the right) as a function of ambient light level (DCO-OFDM). The BER threshold is indicated. Adapted with permission from [72] © The Optical Society.

This behavior was opposite to that of the a-Si module, which systematically showed improved SNR in the presence of ambient lighting, a fact that was not fully understood, but a clear improvement in the *a*-Si module fill factor was observed in the presence of background light. For the first time in the context of VLC applications, the authors also performed impedance spectroscopy measurements to characterize their PV modules, a powerful technique to investigate the capacitive response of devices under dynamic electrical perturbation and under realistic working conditions (dark or under incident light). In this case, as the signal amplitude increases, the SNR improves through a drastic reduction of the effective capacitance of the devices. In 2018, IM2NP Institute in Marseille (France) and SunPartner Technologies developed a dedicated VLC test bench based on OFDM signals to characterize more systematically semi-transparent amorphous silicon modules from SunPartner Technologies [81]. The saturation of different photosensitive

devices (avalanche photodiode—APD, GIGS modules, and a-Si modules) was analyzed, pointing out the exceptional performance of PV devices for OWC in outdoor scenarios, where ambient noise plays an important role in the communication performance. In order to reduce the influence of ambient noise, a receiver design based on two identical a-Si solar panels—one devoted to the reception of ambient noise—was proposed by an Indian team, showing the benefit of the approach [82].

In 2018, a high-performance VLC link and power transfer were demonstrated using a GaAs photovoltaic cell by the University of Edinburgh [83]. In this work, the authors obtained a record power conversion efficiency of at least 42% for their GaAs device acting as a laser power converter (LPC) using a monochromatic VECSEL laser as an emitter at 847 nm. The GaAs PV device bandwidth is measured at 24.5 MHz in this case due to a very small area (1 mm diameter) strongly reducing its capacitive limitation in contrast with larger silicon-based solar panels. Using an OFDM-based VLC system and LOS channel distance of 2 m between the laser emitter and GaAs PV receiver, they achieved a record data rate of 0.5 Gbit/s with a BER of 1.3×10^{-3} under the monochromatic illumination at 0.46 W·cm^{-2} under low load conditions. In 2020, the same group was able to push the performance forward up to a 1 Gbit/s record under short-circuit conditions, while simultaneous energy harvesting led to unprecedented harvested power of 1 mW while ensuring a transmission rate of 784 Mbit/s [84]. In the latter work, Fakidis et al. also analyzed the influence of the modulated signal amplitude (u_g in Figure 5b) on the maximum achievable data rate for an acceptable BER, from which was concluded that the AC amplitude u_g affects only the communication performance of the system. However, the signal amplitude has great impact on different aspects, bringing to the front the flickering behavior of optical sources for great values of u_g. The receiver circuit, as well as data rate and DC electrical current as a function of load voltage (for different AC amplitudes) are given in Figure 5.

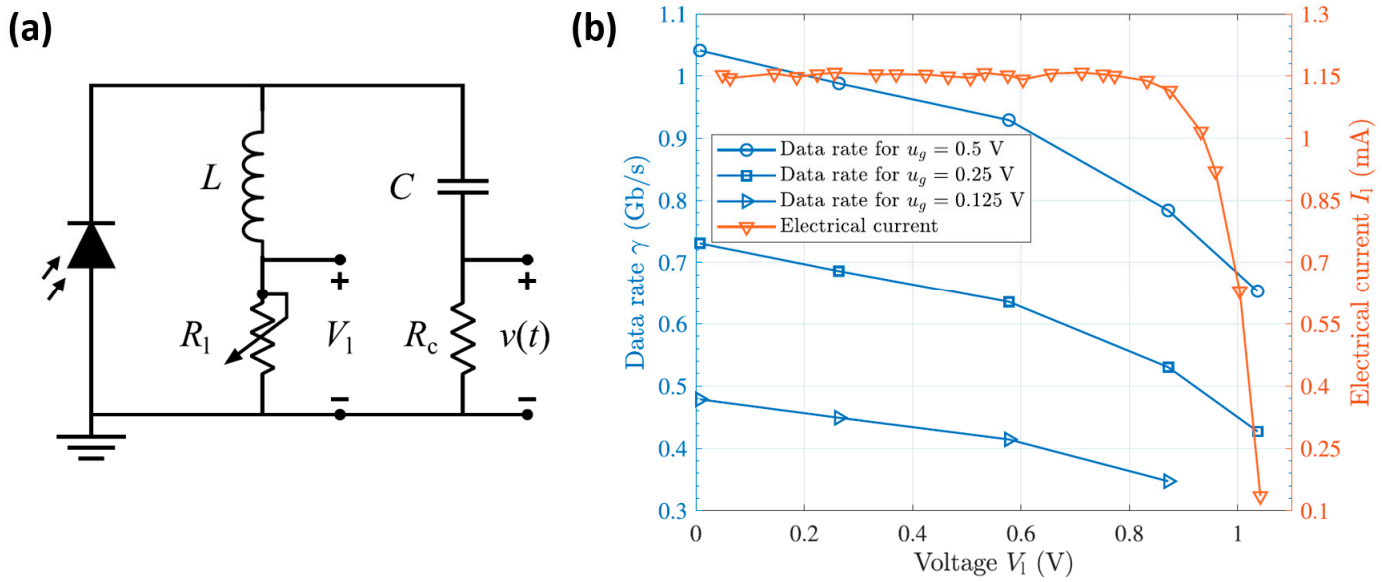

Figure 5. (**a**) Electrical circuit of the GaAs PV-based receiver used in reference [84]. (**b**) Corresponding data rate and DC current as a function of load voltage for an OFDM-based transmission with adaptative bit and power loading. Reproduced with permission from reference [84].

These recorded demonstrations, although realized in ideal laboratory LOS conditions using highly efficient optoelectronic devices for light emission and reception, demonstrate the potential of small-area PV receivers for SLIPT systems.

The dual function of solar cells has also been analyzed for underwater communications where transmission conditions are severe, given the attenuation of the water channel. The results obtained by several authors demonstrate the full extent of the SLIPT concept [85–87].

Apart from these preliminary works, the initial exploitation of solar cells and camera sensors to receive data in simple indoor VLC scenarios involving mobile devices or positioning issues was also demonstrated early in 2016 [88,89], but without focusing on the receiver properties and with no energy harvesting. In fact, the first practical IoT case study was provided by S. Lee in 2015, which proposed a completely autonomous passive transponder using a commercial Si solar panel (11 $\times$ 16.5 cm^2) [64]. The 3 $\times$ 3 white LED array could send a 4.8 kbit/s data rate over a 1 m distance to the receiver, detecting around 5 $mW{\cdot}cm^{-2}$ and generating enough power to supply a microprocessor responsible for sending the feedback signal using another white LED. Although the work does not focus on the SLIPT concept, it is still the first functional system using a PV device for both energy harvesting and data reception. Sometime later, Carrascal et al. developed an on-demand sensor node wake-up using an *a*-Si panel (3.6 $\times$ 2.6 cm^2) that was able to operate autonomously [90]. Despite the fact that it lacks energy harvesting details, the work succeeded in creating a complete VLC system with interesting communication parameters analysis, such as light flickering observation according to the LED's AC component, the necessity to adapt the data rate to the frequency response of PV panels as a function of its size, and also a detailed comparison between frequency responses of the solar panel and a commercial photodiode. Indirectly, this work illustrates the close relationship between the geometric capacitance of the module and its bandwidth through the *RC* limitation.

Three years later, in 2019, Dos et al. brought the SLIPT concept to a whole new level by employing a 1st generation Si panel (30.6 $\times$ 21.8 cm^2) for internet connection under real-world conditions [91]. Although this work was not addressing an indoor scenario, it remains highly relevant to illustrate the relation between device physics and dynamic response. A 2 $\times$ 2 vertical-cavity surface-emitting laser (VCSEL) operating in the infrared (IR) spectrum (940 nm) was placed on top of a lighthouse to implement a 30 m range light-fidelity (LiFi) network for two users. The authors modeled the panel as a PN diode and studied different physical parameters, which are important for both communication and energy harvesting performances. As a matter of fact, the doping ratio of the junction will dictate the thickness of the depletion region, which in its way, directly influences the quantum efficiency and, inversely, the time response of the device. For full collection, the minority charge carriers must cross the depletion region, with associated characteristic times described in Equations (1) and (2) [92]:

$$\tau_h = \frac{W}{\mu_h E} \tag{1}$$

$$\tau_e = \frac{W}{\mu_e E} \tag{2}$$

where τ_h and τ_e are the required time to cross the depletion region for holes and electrons, respectively, W is the depletion region thickness, μ_h and μ_e are the mobility factor for holes and electrons, respectively, and E is the electric field across the device. The intrinsic bandwidth is an important factor that limits communication performance and is inversely proportional to the time response of the device.

We can see that the trade-off between energy harvesting and data reception is driven by the properties of active layer materials, through the doping level of the semiconductors, since thicker depletion region results in higher quantum efficiency but slower devices. After a complete study of the parameters of both the receiver and transmitter and the local climatic scenario, the Scottish team implemented for the first time a free-space optics (FSO) autonomous weather-adaptative system using a PV device, harvesting energy from both IR emitters and solar irradiation. In addition, they achieved an uplink data rate of up to 2.54 Mbit/s and 8.05 Mbit/s for the downlink. This work shows the full potential of PV-based OWC systems for SLIPT scenarios.

We, finally, propose a synthetic summary of the most impactful experimental contributions reported to date in this field using Si-based and thin film PV technologies (see

Table 2). We highlight the best performance obtained regarding energy harvesting and data reception, even though some of them were obtained under different conditions.

Table 2. Summary of some of the most impactful contributions for SLIPT-based systems (with 1st and 2nd generation of PV devices) with their respective information about the illumination, receiver characteristics (PV technology, type of device, and active area size), experiment condition (type of link and distance between Tx and Rx), energy harvesting parameters (PCE and output power), communication performance (bandwidth and data rate), and most notable feature.

Ref	Illumination	Receiver Type Active Area	Experiment Conditions	Energy Harvesting Performance (PCE and Output Power)	Communication Performance (Bandwidth and Data Rate)	Particularity
[61] 2014	Solar + White LED	Si cell 7.29 cm^2	Indoor LOS SISO 40 cm	16% PCE 43.81 mW	10 kHz 3 kbit/s	First proof of concept
[62] 2014	White LED	Si module 432 cm^2	Indoor LOS SISO 24 cm	2.1 mW	350 kHz 7.01 Mbit/s	First proof of concept using one source to send data and energy
[63] 2015	White LED	Si module 432 cm^2	Indoor LOS SISO	30 mW	350 kHz 11.84 Mbit/s	First circuit for simultaneous data reception and energy harvesting
[64] 2015	White LED array	Si module 181.5 cm^2	Indoor LOS SISO Real-life context 1 m	Supply the reception circuit	15 kHz 4.8 kbit/s	First real-life scenario SLIPT system
[90] 2016	White LED	α-Si module 9.36 cm^2	Indoor LOS SISO Real-life context 60 cm	Supply the reception circuit	2 kbit/s	Performance comparison with photodiode
[75] 2016	White LED	Si module 42.35 cm^2	Indoor LOS SISO 10 cm	26% PCE	120 kHz 17.05 Mbit/s	First self-biased architecture
[89] 2016	3 White LEDs	α-Si cell 27.1 cm^2	Indoor LOS MISO ~2 m	Autonomous receiver	2 kbit/s	Only positioning system with PV receiver
[77] 2017	2 White LEDs	α-Si cell 27.1 cm^2	Indoor LOS SISO 1.5 m	N/A	1 Mbit/s	First use of pre-distortion to improve PV receiver performance
[83] 2018	Infrared laser	GaAs cell 0.78 mm^2	Indoor LOS SISO 2 m	42% PCE 1.5 mW (obtained over 1 mm)	24.5 MHz 522.1 Mbit/s	Proof of concept of high communication performance for small surface PV device
[81] 2018	White LED	CIGS and α-Si modules	Indoor LOS SISO	N/A	Bandwidth analysis	Illumination and material influence on the bandwidth
[85] 2019	Solar + White laser	α-Si module 144 cm^2	Indoor Outdoor LOS SISO 20 m	474 mW (solar power)	290 kHz 1 Mbit/s	Include first underwater scenario
[91] 2019	Solar + Infrared laser	Si module 667.08 cm^2	Outdoor LOS SISO Real-life context 30 m	12.5% PCE 5 W	270 kHz 8 Mbit/s	First PV-based system for internet under real-world conditions
[84] 2020	Infrared laser	GaAs cell 0.78 mm^2	Indoor LOS SISO 40 cm	41.7% PCE 0.98 mW	24.5 MHz 1041 Mb/s	Record data rate at SLIPT scenario

Table 2. *Cont.*

Ref	Illumination	Receiver Type Active Area	Experiment Conditions	Energy Harvesting Performance (PCE and Output Power)	Communication Performance (Bandwidth and Data Rate)	Particularity
[93] 2020	Solar + While LED	CIGS module 26.05 cm^2	Outdoor LOS SISO 23 cm	N/A	Error-free maximum frequency analysis	Comparison between PD and CIGS PV in outdoor scenario
[94] * 2021	White LED	Si module 100 cm^2	Indoor LOS SISO	Theoretical values	Capacity bound analysis	Optimization procedure according to receiver battery status
[95] 2021	White LED	Si module	Indoor LOS SISO 1 m	N/A	Multiple performance for multiple light intensity	First characterization of the non-linear aspect of PV devices
[76] 2021	Red LED	GaAs cell 9 cm^2	Indoor LOS SISO 32.5 cm	347 µW	2.5 kbit/s	Dense analysis of the reception circuit
[96] 2021	Solar + Infrared laser	Si module 667.08 cm^2	Indoor LOS SISO 3.5 m	4.5 W	6.34 Mbit/s	First use of double diode model for communication analysis

* Article purely theoretical.

2.3. Harvesting Energy and Data Using Emerging PV Technologies

Even before the first simultaneous energy harvesting and data reception proposal, the potential of the third generation of PV cells for communications (with no energy harvesting) had already been inspected; the authors referred to their devices as photodetectors [97–99]. However, the devices are made of PV-based architecture, mainly fabricated for energy harvesting purposes, but were negatively (or zero) biased, denying their power collection capabilities. Although these works do not consider simultaneous energy harvesting, they actually highlight the impressive dynamic characteristics of emerging PV devices.

Not much longer from the first proof of concept reported in [61–63], the high power conversion efficiencies of emerging PV technologies under indoor environments brought up fascinating questions concerning their communication performances in SLIPT contexts. As early as mid-2015, Zhang et al. used a state-of-the-art organic solar cell for simultaneous energy harvesting and data reception [100]. The 8 mm^2 OPV, based on PTB7:PC_{71}BM active layer, performed amazingly well, achieving a 7% PCE under AM 1.5G solar simulator, with a 0.75 V V_{OC}, a 14.6 mA/cm^2 J_{SC} and a FF of 63.8% [101]. It was then attached to the first ever developed reception circuit [63] (as shown in Figure 2b) and, using a red LD with 8.5 mW output power over a 1 m distance, the OFDM-based system reached 34.2 Mbit/s with 4.08 $\times$ 10^{-4} BER at the MPP, while generating 0.43 mW output electrical power. This was, in fact, the first PV-based VLC system that achieved data rates higher than 12 Mbit/s, but the reason why it performed better is still a question. One may deduce that greater data rates came with the smaller active area of the device, implying a reduced geometric capacitance and, finally, a reduced response time, while others claim that the drift velocity of organic materials is higher than the ones found in Si-based materials [102,103], resulting in an increase in the receiver's bandwidth. However, no detailed studies have been proposed since then.

Some years later, in 2019, a French team performed communication tests on a module composed of 9 ASCA® OPV cells in series developed by Armor Company (Nantes, France) [104,105]. Although Lorrière et al. did not carry out any energy harvesting experiments, they considered some interesting characteristics of OPV modules to measure their bandwidth, such as the operating point, the influence of the DC illumination, and the effects of shading. In a no-DC illumination scenario (only AC component present at the signal), the short circuit condition performed 50 times better than in open circuit, achieving 66.4 kHz and 1.3 kHz for I_{SC} and V_{OC}, respectively. Interestingly, increasing the LED's DC radiation decreased the bandwidth of the device for V_{oc} measurement, while slightly increasing the

communication performance under short circuit condition, behavior contradictory to the one seen in previous reports [93,96]. The French team was also able to analyze the bandwidth on controlled masking. When all solar cells of the module are partially covered, the masking physically acts by reducing the total active surface of the PV device and, therefore, proportionally, the generated current. Therefore, the bandwidth is reduced. However, fully covering a solar cell of the module results in an increase in the load observed for the series-connected uncovered cells, leading to a band-pass filter behavior [106].

The first ever PSC-based OWC system was recently proposed by Mica et al., which developed triple-cation PV devices for telecommunication purposes while simultaneously harvesting energy [107]. The active layer based on Cesium-containing perovskite, first reported for photovoltaic application [108], was chosen by the authors for its high PCE and good bandwidth. The device was optimized for VLC goals by changing the active layer thickness between 60 and 965 nm, which in its own way affects both energy harvesting and communication performances of the PV cell, characteristics that were experimentally measured separately. Using a white LED with 0.9 mW·cm^{-2} incident optical power, the average PCE of the devices increases with the thickness of the active layer, achieving its maximum value at 21.4% for a thickness of 640 nm, before decreasing for thicker layers. Both FF and V_{OC} show a significant improvement when the thickness of the perovskite layer expands, but drop drastically for 840 nm and 965 nm, as a result of enhanced charge recombination at the perovskite/hole transport material interface [107]. Although the energy harvesting performance was measured using a white LED, a red LD was used for data transmission. Regarding communication performance, the bandwidth of the device also improves with thicker active layers, reaching its maximum value of 586 kHz at 965 nm (measured in short circuit condition), as can be seen in Figure 6a. Mica et al. performed a careful analysis to find the physical cause of the bandwidth behavior, observing that thicker perovskite resulted in lower geometric capacitance C, while sustaining an acceptable effective resistance R (see Figure 6b). Interestingly, they confirmed the RC time constant through transient photovoltage measurements, showing a nice consistency with the frequency-dependent measurements. Despite the fact that thicker PSC allowed larger bandwidths, the achievable data rate in OFDM-based schemes depends on each subcarrier rather than on the cutoff frequency of the device, a reason why the receiver based on a 250 nm perovskite active layer achieved the maximum data rate of 56 Mbit/s (3×10^{-3} BER over 40 cm), which is still the highest value reported in the literature for a perovskite solar cell. In fact, this is the first work performing a detailed analysis of the influence of the solar cell architecture on its energy harvesting and communication performance.

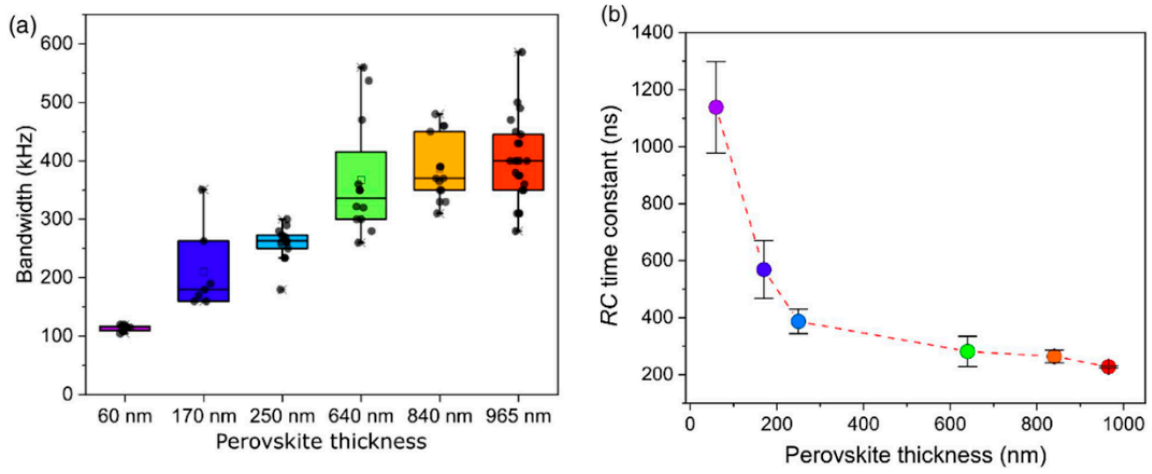

Figure 6. (**a**) Obtained bandwidth in function of perovskite thickness; (**b**) Measured RC constant for solar cells with different perovskite thickness. Reproduced with permission from [107].

The influence of the device architecture on communication performance drew the attention of both physics and telecommunications communities. In 2021, Tavakkolnia et al. further exploited the concept by developing the first multiple-input multiple-output (MIMO) system based on an OPV device for SLIPT purposes [109]. In this work, the authors reported the use of an inverted OPV device architecture (or *n-i-p*) [110], well-known in the photovoltaic community, to address the intrinsic degradation of regular architectures (referred to as *p-i-n* architecture). Targeting improved lifetime of OPV-based systems, Tavakkolnia et al. also explored different acceptor/donor combinations in order to better match the artificial light source spectrum. In this work, the active layer was composed of highly efficient polymer donors (PTB7 or PTB7-Th) and fullerene or non-fullerene electron acceptors (namely $PC_{71}BM$ or EH-IDTBR). The optical absorption of fullerene acceptors is indeed not adapted to indoor lighting, and shifting from $PC_{71}BM$ to EH-IDTBR resulted in better energy harvesting efficiency [111]. The OPV devices were composed of multiple individual 10 mm^2 pixels, allowing independent data extraction for single-input single-output (SISO) or MIMO analysis by combining up to 8 pixels. Similarly to [107], the energy harvesting investigation was realized using a white LED with a 5.9 $mW{\cdot}cm^{-2}$ irradiation, while communication scenarios were performed using a 56.2 mW red laser (placed 40 cm away from the receiver) and concentrating lens.

In order to compare the performance of each active layer separately, initial tests in a SISO configuration were realized. Table 3 shows the PCE of solar cells under white LED, the measured bandwidth, the generated power when aligned with the red LD, and the obtained data rate. Each data rate corresponds to BER low enough for error-free transmission with forward error correction. As expected, the non-fullerene-based OPV performed better in indoor lighting conditions when compared to $PC_{71}BM$. In fact, 147.5 Mbit/s is the highest data rate achieved with a single OPV cell in the literature.

Table 3. Obtained communication and indoor energy harvesting performances for different OPVs in a SISO configuration. Adapted with permission from reference [109].

	PCE (White LED)	Bandwidth (MHz)	Harvested Power (mW)	Data Rate (Mbit/s)
PTB7:$PC_{71}BM$	—	1.32	3.3	90.3
PTB7-Th:$PC_{71}BM$	10.9%	1.26	3.5	78.4
PTB7-Th:EH-IDTBR	14.1%	2.77	3.7	147.5

To further improve the performance of their work, the authors developed a MIMO VLC system using four OPVs and four LDs, which brings up different challenges, such as inter-channel cross-talk. With the PTB7-Th:EH-IDTBR device, the data rate was pushed up to 363 Mbit/s while simultaneously harvesting 10.9 mW, a high power in the context of VLC for IoT.

Despite the fact that all aforementioned experiments were conducted in ideal LOS scenarios, they constitute the first proof of concept of emerging PV devices for SLIPT purposes and demonstrate the feasibility of developing indoor IoT devices with partial or full autonomy.

We propose a synthetic approach containing all SLIPT works based on emerging PV technologies, highlighting some important energy harvesting and communication parameters, as well as the most notable feature of the article (see Table 4). By separating the references into emerging PV technology and 1st and 2nd generations, we bring the innovative, dynamic aspect of the 3rd generation to the fore, pointing out the lack of works that analyze the physical property and achievable performance of these ingenious multi-layer devices.

Table 4. Summary of some of the most impactful contributions for SLIPT-based systems (with emerging PV technologies) with their respective information about the illumination, receiver characteristics (PV technology, type of device, and active area size), experiment condition (type of link and distance between Tx and Rx), energy harvesting parameters (PCE and output power), communication performance (bandwidth and data rate), and most notable feature.

Ref	Illumination	Receiver Type Active Area	Experiment Conditions	Energy Harvesting Performance (PCE and Output Power)	Communication Performance (Bandwidth and Data Rate)	Particularity
[100] 2015	Red laser	OPV cell 8 mm^2	Indoor LOS SISO 1 m	0.43 mW	1.3 MHz 42.3 Mbit/s	First SLIPT system with OPV
[105] 2019	White LED	OPV module 57.2 cm^2	Indoor LOS SISO	N/A	Bandwidth analysis	Shadowing influence on the bandwidth
[107] 2020	White LED + Red laser	Perovskite cell 6.5 mm^2	Indoor LOS SISO 40 cm	21.4% PCE (LED) 3.3 mW (laser)	586 kHz 56 Mb/s	Active layer thickness influence on communication parameters
[109] 2021	White LED + Visible laser	OPV cell 10 mm^2 40 mm^2 (MIMO)	Indoor LOS SISO MIMO 40 cm	14% PCE (LED) 10.9 mW (laser)	2.77 MHz 363 Mbit/s (MIMO)	Record data rate at SLIPT scenario with OPV and active layer material comparison

Regarding emerging PV devices, we also emphasize a specific feature of the technologies in direct relation to the proposed application. Indeed, both OPV and PSC share a multi-layered architecture where several thin films of various natures are vertically stacked. Interfacial engineering is shown to be a crucial challenge for photovoltaic energy conversion for OPV [112] and PSC [113], as interfacial defects are easily introduced during solution-based processing steps. While they clearly alter the steady-state properties of the devices, they are also crucial for the dynamics of the electrical response under modulated optical signals through additional capacitive contributions. Especially, such interfacial processes are expected to contribute to the high-frequency response of the device, either through specific interfacial RC limitations (in case of relatively "slow" processes due to charge trapping/detrapping, charge accumulation, or charge recombination) or even through additional contribution to the geometric capacitance, as was emphasized in some studies [107]. We believe that impedance spectroscopy is a relevant tool to discriminate the associated mechanisms [80,114] better and that interfacial engineering is also an additional lever to tune the bandwidth of emerging PV devices [115]. In any case, bandwidth modulation of emerging PV modules is a crucial challenge toward efficient data and energy harvesting in the future.

2.4. Lessons Learned on the Trade-Off between Energy Harvesting and Data Reception: Operating Point Dependence

Most of the aforementioned reports emphasized the close relationship between energy harvesting and data reception efficiencies. Clearly, from the initial receiver circuit proposed to decouple the DC (energy) and AC (data) components using dedicated capacitive and inductive branches (see Figure 2b), one can rapidly evidence the impact of equivalent circuit components such as resistances (R_L and R_C) on photo-generated power and data rate in a specific scenario. Moreover, both the working point of the steady-state I(V) characteristics (hence the power generation efficiency) and the effective capacitance of the device (hence its dynamic response) depend on the operating voltage V, which in turn, depends on the values of the equivalent circuit components. It turns out that the communication branch of the proposed circuit (i.e., C_0 and R_c in Figure 2b) does not affect in any way the energy harvesting performance of the receiver [63]. However, the energy harvesting branch defines the operating voltage V of the solar cell, influencing both recovered power and data reception. This is the reason why harvested power and data rate curves are intimately bound (as in Figure 5b). Various research have illustrated the influence of the

operating point on the bandwidth, linearity and responsivity of the PV device. Short circuit condition provides the best communication performance, and linearity between the output current and the input AC irradiation, while increasing the output voltage decreases the data reception capabilities, but increases the power collection of the receiver [75,76,83,84,87].

These features and the underlying trade-offs are discussed in more detail in a recent article by Sepehrvand et al., which shows how the DC operating point of the device can be selected using a power converter—a technique that was first discussed by Shin et al.—so that the harvested power and data rate can be tuned as a function of the real-time needs of VLC systems [94]. Their analysis points out the voltage dependence of the total capacity of the device, which is derived from both the depletion capacitance (separation of positive and negative charges in the depletion region) and the diffusion capacitance (which originates from the stored minority carriers near the depletion region). By proposing an optimization procedure, they suggest a generic analytical framework to select the best working point of solar panels used as VLC receivers in indoor IoT scenarios. Such considerations will be extended in the next section devoted to emerging PV devices used for VLC applications.

2.5. Considerations on the Influence of Illumination Conditions and Ambient Noise

A fundamental question on the use of solar panels for VLC reception is associated with the device's behavior as a function of illumination intensity and noise level. The performance of a VLC system was measured by comparing a traditional APD and a CIGS module from Solar Frontier (26 cm^2) solar panels, both placed under variable illumination conditions, from indoor to outdoor [93]. Interestingly, for sunlight exposure as low as 200 W/m^2, the APD showed a clear saturation effect which limits the data rate down to a few tens of kHz. In contrast, the CIGS PV module still showed an acceptable BER up to 400 kHz under full sun illumination (1000 $W \cdot m^{-2}$). Such considerations are relevant in indoor scenarios where IoT nodes will operate near an important source of light noise.

Similar considerations were also dedicated to silicon-based PV modules placed under various ambient light intensities, using a modulated laser diode (LD) at 940 nm and a DCO-OFDM scheme for communication purposes [96]. Using a two-diode equivalent circuit to model the junction recombination occurring under low illumination, as well as thermal, dark, and shot noises, they were able to model the frequency response of their solar panel and compare it to experimental measurements, which showed very good agreement between theory and experiment. The authors also analyzed the influence of the irradiation level on both data rate and harvested power. Das et al. experimentally showed that as ambient noise increases, the PV device bandwidth decreases, a behavior that is consistent with that observed for CIGS modules in [93]. Again, the trade-off between data rate and power is defined by the receiver's electrical components, which govern the operation conditions of the device.

Another aspect that should be mentioned in the case of PV receivers is the non-linear distortions that appear at low illumination conditions on the output voltage of the device, specifically in indoor environments (<1000 Lux). Indeed, solar cells show a logarithmic dependence of voltage with irradiance level when driven in non-reverse bias conditions, as can be seen in Equation (3) [116]:

$$V \approx \frac{nk_BT}{q} \ln\left(\frac{I_{PH}}{I_0} + 1\right) \quad (3)$$

where V is the voltage of the load, I_{PH} the generated photocurrent, I_0 the reverse saturation current of the diode of ideality factor n, k_B the Boltzmann's constant, T the temperature, and q the elementary charge. I_{PH} being linearly proportional to the light intensity, Equation (3) shows that non-linear effects are expected in the electrical conversion of photons to electrons at low light intensity. Such effects were quantified by theoretical and experimental comparisons by the Chinese University of Hong Kong in 2021 using a commercial monocrystalline silicon cell [95]. Specific distortions can be observed below 1000 Lux, leading to BER degradation. Be that as it may, while this effect remains to be considered at low illumi-

nation conditions, specific post-distortion compensation schemes can be used to improve communication performance at non-linear operation regions.

3. Discussion and Conclusions

In this article, we summarized different aspects of PV devices for indoor applications, notably their energy harvesting and data reception performances in a SLIPT scenario. We first highlight the high-power conversion efficiencies of emerging PV technologies (DSSC, OPV, and perovskite) under artificial light sources, compared to inorganic or thin film technologies. Such performance, coupled with their intrinsic tunability in terms of electronic properties, their high specific power, and their high flexibility, make them very good candidates for answering the contemporary ecological challenges of the next generation of Green IoT systems. The modern SLIPT concept, which aims at simultaneously allowing energy harvesting and optical wireless data reception using a single photovoltaic device, brings different challenges for the scientific community, mainly associated with the dynamic response of solar cells, which are currently not fully investigated.

Since the first proposal of the reception circuit by Wang et al., the community has been interested in the development of more complex front-ends at the receiver side, emphasizing the importance of electronics for both communication and energy harvesting. Different architectures were proposed, bringing to the fore the works described in [76,94], which provide real-time solutions for the energetic challenges of IoT nodes. However, each work proposed a front-end with a constant load that allows maximum efficiency of the PV device, without considering more complex energy harvesting electronic techniques, for instance, maximum power point tracking (MPPT), which is highly required in modern PV systems [117]. By proposing the replacement of the constant charge R_L (see Figure 2b) with a more complex circuit, the communication branch that allows simultaneous data reception is directly affected. This, in fact, shows the innovative aspect of the SLIPT notion and the lack of works about the electronics of the concept. Ultimately, demonstrating a relevant electronic receiver circuit able to tune the real-time load conditions to account for the best trade-off between energy harvesting and data reception (in terms of quality of service based on specific performance indicators) would be highly relevant for this application, and we can only invite the community to tackle this challenge.

From the proof of concept and beyond, most works tried to characterize the PV device from the communication side, extracting the best performance (bandwidth and data rate) using state-of-the-art technologies in a direct LOS scenario. We highlighted some works that achieved unprecedented communication performances with simultaneous energy harvesting, such as [79,83,84,109], which not only show the feasibility of SLIPT systems but demonstrate their high adaptation capability according to different IoT impositions. However, to allow deployment in realistic indoor environments, research is still needed for more complex configurations involving NLOS links. Some impactful concerns associated with indoor situations were also discussed in very few papers, from which we can highlight the crucial impact of ambient noise (such as sunlight or other undesired artificial sources), which can improve the collected energy but can also limit the communication performance according to the technology. Lorrière et al. experimentally demonstrated the increase in bandwidth for a CIGS device when ambient noise increases, while Das et al. showed that the opposite occurs for Si-based devices. This accentuates the lack of research introducing comparative experiments with different technologies of PV cells.

The influence of shadowing on the communication performance was inspected only in a single work [105], detailing interesting characteristics for different scenarios, namely the pass-band feature of the module when sub-cells are fully masked. As a matter of fact, understanding the physical and communication behaviours of modules is complex, and no works can be found about their dynamic characterization.

Some reports emphasize the impact of the PV technology employed, inspecting the influence of both active layer physical properties and device architecture on the bandwidth [107,109], but no deep comparative studies were performed. The size of the active

area of the photovoltaic device was shown to play an important role in its optoelectrical conversion efficiency, i.e., a larger active area collects more optical power, but they are associated with larger junction capacitance, which limits the response time. From two articles published in 2020 [79,84], we can notice a great difference between communication performances: one work achieved 74.03 Mb/s with a 667 cm^2 Si module, while the other obtained 1041 Mb/s with a 1 mm diameter GaAs solar cell (both under same operation voltage). We can clearly see the active area's influence on the dynamic limitations, but the influence of the technology is still uncertain.

Figure 7 synthesizes the maximum measured bandwidth and obtained data rates as a function of the device's active area based on a first-level literature survey. In fact, as detailed in Sections 2.3 and 2.4, the bandwidth also depends on the bias applied at the PV cell and on the illumination condition. The maximum obtained data rate also depends on the employed modulation scheme, for instance, multicarrier modulations (OFDM), which perform better than the basic OOK but involve more complex systems, which are not necessarily compatible with IoT uses at low consumption and do not require high rates. The geometric capacitance influence on the bandwidth can be noticed since a smaller surface area tends to decrease the response time of the device. However, for a more direct conclusion, both communication parameters should be obtained at the same testing condition.

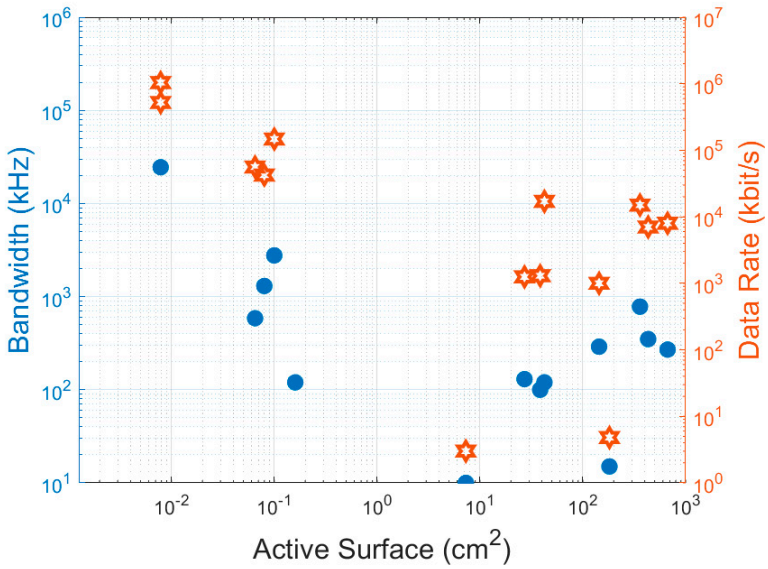

Figure 7. Measured bandwidth and data rate for PV devices with different active surfaces. Data obtained from references [61,62,64,71,75,78,83–85,87,91,99,100,107,109].

Tables 2 and 4 illustrate the true potential of photovoltaic devices for energy harvesting and data reception, going from outdoor to indoor scenarios. This survey also emphasizes that most of the research efforts remain focused on LOS configurations based on direct incidence and on short distances, using off-of-the-shelf PV devices. However, the realistic deployment of SLIPT systems for IoT will require accounting for NLOS paths, including multiple reflections from the environment, potential obstacles associated with mobility scenarios, and the consideration of multiple noise sources. The real performance of PV modules of complex shapes integrated on curved surfaces is particularly difficult to predict in such environments. The energy harvesting and data reception performances of third-generation PV devices, which typically target scenarios for the smart home, smart factory, or wearable electronics, will strongly depend on the complexity of the environment, and innovative simulation tools will be crucial for practical applications.

In any case, although the SLIPT concept constitutes a relatively new field of investigation, it obviously shows a true potential to address several crucial challenges associated with the next generation of the digital ecosystem.

Author Contributions: J.B., D.R.D.S. and A.J.-V. equally contributed to the preparation of the article. All authors have read and agreed to the published version of the manuscript.

Funding: This research was funded by the French "Ministère de l'Enseignement Supérieur et de la Recherche" and the IoT-PV Régional project (Région Nouvelle Aquitaine, grant number AAPR2021A-2020-12033410). The authors are grateful to the CASI board at XLIM for financial support.

Institutional Review Board Statement: Not applicable.

Informed Consent Statement: Not applicable.

Data Availability Statement: Not applicable.

Conflicts of Interest: The authors declare no conflict of interest. The funders had no role in the design of the study; in the collection, analyses, or interpretation of data; in the writing of the manuscript; or in the decision to publish the results.

References

1. *Renewables 2021—Analysis and Forecast to 2026*; International Energy Agency: Paris, France, 2021; p. 175.
2. Victoria, M.; Haegel, N.; Peters, I.M.; Sinton, R.; Jäger-Waldau, A.; del Cañizo, C.; Breyer, C.; Stocks, M.; Blakers, A.; Kaizuka, I.; et al. Solar Photovoltaics Is Ready to Power a Sustainable Future. *Joule* **2021**, *5*, 1041–1056. [CrossRef]
3. Study: Levelized Cost of Electricity—Renewable Energy Technologies—Fraunhofer ISE. Available online: https://www.ise.fraunhofer.de/en/publications/studies/cost-of-electricity.html (accessed on 21 June 2022).
4. Timilsina, G.R. Are Renewable Energy Technologies Cost Competitive for Electricity Generation? *Renew. Energy* **2021**, *180*, 658–672. [CrossRef]
5. Almora, O.; Baran, D.; Bazan, G.C.; Berger, C.; Cabrera, C.I.; Catchpole, K.R.; Erten-Ela, S.; Guo, F.; Hauch, J.; Ho-Baillie, A.W.Y.; et al. Device Performance of Emerging Photovoltaic Materials (Version 2). *Adv. Energy Mater.* **2021**, *11*, 2102526. [CrossRef]
6. Bae, S.-H.; Zhao, H.; Hsieh, Y.-T.; Zuo, L.; De Marco, N.; Rim, Y.S.; Li, G.; Yang, Y. Printable Solar Cells from Advanced Solution-Processible Materials. *Chem* **2016**, *1*, 197–219. [CrossRef]
7. Nayak, P.K.; Mahesh, S.; Snaith, H.J.; Cahen, D. Photovoltaic Solar Cell Technologies: Analysing the State of the Art. *Nat. Rev. Mater.* **2019**, *4*, 269–285. [CrossRef]
8. Liu, H.; Yu, M.-H.; Lee, C.-C.; Yu, X.; Li, Y.; Zhu, Z.; Chueh, C.-C.; Li, Z.; Jen, A.K.-Y. Technical Challenges and Perspectives for the Commercialization of Solution-Processable Solar Cells. *Adv. Mater. Technol.* **2021**, *6*, 2000960. [CrossRef]
9. Wang, X.; Sun, Q.; Gao, J.; Wang, J.; Xu, C.; Ma, X.; Zhang, F. Recent Progress of Organic Photovoltaics with Efficiency over 17%. *Energies* **2021**, *14*, 4200. [CrossRef]
10. Wu, T.; Qin, Z.; Wang, Y.; Wu, Y.; Chen, W.; Zhang, S.; Cai, M.; Dai, S.; Zhang, J.; Liu, J.; et al. The Main Progress of Perovskite Solar Cells in 2020–2021. *Nano-Micro Lett.* **2021**, *13*, 152. [CrossRef] [PubMed]
11. Azmi, R.; Ugur, E.; Seitkhan, A.; Aljamaan, F.; Subbiah, A.S.; Liu, J.; Harrison, G.T.; Nugraha, M.I.; Eswaran, M.K.; Babics, M.; et al. Damp Heat–Stable Perovskite Solar Cells with Tailored-Dimensionality 2D/3D Heterojunctions. *Science* **2022**, *376*, 73–77. [CrossRef]
12. Reich, N.H.; van Sark, W.G.J.H.M.; Turkenburg, W.C. Charge Yield Potential of Indoor-Operated Solar Cells Incorporated into Product Integrated Photovoltaic (PIPV). *Renew. Energy* **2011**, *36*, 642–647. [CrossRef]
13. Biswas, S.; Kim, H. Solar Cells for Indoor Applications: Progress and Development. *Polymers* **2020**, *12*, 1338. [CrossRef]
14. Li, M.; Igbari, F.; Wang, Z.-K.; Liao, L.-S. Indoor Thin-Film Photovoltaics: Progress and Challenges. *Adv. Energy Mater.* **2020**, *10*, 2000641. [CrossRef]
15. Cao, Y.; Liu, Y.; Zakeeruddin, S.M.; Hagfeldt, A.; Grätzel, M. Direct Contact of Selective Charge Extraction Layers Enables High-Efficiency Molecular Photovoltaics. *Joule* **2018**, *2*, 1108–1117. [CrossRef]
16. Ma, L.-K.; Chen, Y.; Chow, P.C.Y.; Zhang, G.; Huang, J.; Ma, C.; Zhang, J.; Yin, H.; Hong Cheung, A.M.; Wong, K.S.; et al. High-Efficiency Indoor Organic Photovoltaics with a Band-Aligned Interlayer. *Joule* **2020**, *4*, 1486–1500. [CrossRef]
17. Dong, C.; Li, X.-M.; Ma, C.; Yang, W.-F.; Cao, J.-J.; Igbari, F.; Wang, Z.-K.; Liao, L.-S. Lycopene-Based Bionic Membrane for Stable Perovskite Photovoltaics. *Adv. Funct. Mater.* **2021**, *31*, 2011242. [CrossRef]
18. Hou, B.; Kim, B.-S.; Lee, H.K.H.; Cho, Y.; Giraud, P.; Liu, M.; Zhang, J.; Davies, M.L.; Durrant, J.R.; Tsoi, W.C.; et al. Multiphoton Absorption Stimulated Metal Chalcogenide Quantum Dot Solar Cells under Ambient and Concentrated Irradiance. *Adv. Funct. Mater.* **2020**, *30*, 2004563. [CrossRef]
19. Guo, J.; Min, J. A Cost Analysis of Fully Solution-Processed ITO-Free Organic Solar Modules. *Adv. Energy Mater.* **2019**, *9*, 1802521. [CrossRef]
20. Song, Z.; McElvany, C.L.; Phillips, A.B.; Celik, I.; Krantz, P.W.; Watthage, S.C.; Liyanage, G.K.; Apul, D.; Heben, M.J. A Technoeconomic Analysis of Perovskite Solar Module Manufacturing with Low-Cost Materials and Techniques. *Energy Environ. Sci.* **2017**, *10*, 1297–1305. [CrossRef]
21. Qiu, L.; Ono, L.K.; Qi, Y. Advances and Challenges to the Commercialization of Organic–Inorganic Halide Perovskite Solar Cell Technology. *Mater. Today Energy* **2018**, *7*, 169–189. [CrossRef]

22. Li, Z.; Zhao, Y.; Wang, X.; Sun, Y.; Zhao, Z.; Li, Y.; Zhou, H.; Chen, Q. Cost Analysis of Perovskite Tandem Photovoltaics. *Joule* **2018**, *2*, 1559–1572. [CrossRef]
23. Rabaia, M.K.H.; Abdelkareem, M.A.; Sayed, E.T.; Elsaid, K.; Chae, K.-J.; Wilberforce, T.; Olabi, A.G. Environmental Impacts of Solar Energy Systems: A Review. *Sci. Total Environ.* **2021**, *754*, 141989. [CrossRef] [PubMed]
24. Tian, X.; Stranks, S.D.; You, F. Life Cycle Assessment of Recycling Strategies for Perovskite Photovoltaic Modules. *Nat. Sustain.* **2021**, *4*, 821–829. [CrossRef]
25. Anctil, A.; Lee, E.; Lunt, R.R. Net Energy and Cost Benefit of Transparent Organic Solar Cells in Building-Integrated Applications. *Appl. Energy* **2020**, *261*, 114429. [CrossRef]
26. Venkateswararao, A.; Ho, J.K.W.; So, S.K.; Liu, S.-W.; Wong, K.-T. Device Characteristics and Material Developments of Indoor Photovoltaic Devices. *Mater. Sci. Eng. R Rep.* **2020**, *139*, 100517. [CrossRef]
27. Li, B.; Hou, B.; Amaratunga, G.A.J. Indoor Photovoltaics, the Next Big Trend in Solution-Processed Solar Cells. *InfoMat* **2021**, *3*, 445–459. [CrossRef]
28. Cutting, C.L.; Bag, M.; Venkataraman, D. Indoor Light Recycling: A New Home for Organic Photovoltaics. *J. Mater. Chem. C* **2016**, *4*, 10367–10370. [CrossRef]
29. Freunek, M.; Freunek, M.; Reindl, L.M. Maximum Efficiencies of Indoor Photovoltaic Devices. *IEEE J. Photovolt.* **2013**, *3*, 59–64. [CrossRef]
30. Ho, J.K.W.; Yin, H.; So, S.K. From 33% to 57%—An Elevated Potential of Efficiency Limit for Indoor Photovoltaics. *J. Mater. Chem. A* **2020**, *8*, 1717–1723. [CrossRef]
31. Mathews, I.; Kantareddy, S.N.; Buonassisi, T.; Peters, I.M. Technology and Market Perspective for Indoor Photovoltaic Cells. *Joule* **2019**, *3*, 1415–1426. [CrossRef]
32. Politi, B.; Parola, S.; Gademer, A.; Pegart, D.; Piquemil, M.; Foucaran, A.; Camara, N. Practical PV Energy Harvesting under Real Indoor Lighting Conditions. *Sol. Energy* **2021**, *224*, 3–9. [CrossRef]
33. Devadiga, D.; Selvakumar, M.; Shetty, P.; Santosh, M.S. Dye-Sensitized Solar Cell for Indoor Applications: A Mini-Review. *J. Electron. Mater.* **2021**, *50*, 3187–3206. [CrossRef]
34. Alkhalayfeh, M.A.; Abdul Aziz, A.; Pakhuruddin, M.Z.; Katubi, K.M.M.; Ahmadi, N. Recent Development of Indoor Organic Photovoltaics. *Phys. Status Solidi* **2022**, *219*, 2100639. [CrossRef]
35. Muhammad, B.T.; Kar, S.; Stephen, M.; Leong, W.L. Halide Perovskite-Based Indoor Photovoltaics: Recent Development and Challenges. *Mater. Today Energy* **2022**, *23*, 100907. [CrossRef]
36. Internet of Things (IoT) Market (2021–26) | Industry Size, Growth, Trends—Mordor Intelligence. Available online: https://www.mordorintelligence.com/industry-reports/internet-of-things-moving-towards-a-smarter-tomorrow-market-industry (accessed on 19 October 2021).
37. Ma, D.; Lan, G.; Hassan, M.; Hu, W.; Das, S.K. Sensing, Computing, and Communications for Energy Harvesting IoTs: A Survey. *IEEE Commun. Surv. Tutor.* **2020**, *22*, 1222–1250. [CrossRef]
38. Pecunia, V.; Occhipinti, L.G.; Hoye, R.L.Z. Emerging Indoor Photovoltaic Technologies for Sustainable Internet of Things. *Adv. Energy Mater.* **2021**, *11*, 2100698. [CrossRef]
39. Sanislav, T.; Mois, G.D.; Zeadally, S.; Folea, S.C. Energy Harvesting Techniques for Internet of Things (IoT). *IEEE Access* **2021**, *9*, 39530–39549. [CrossRef]
40. Panidi, J.; Georgiadou, D.G.; Schoetz, T.; Prodromakis, T. Advances in Organic and Perovskite Photovoltaics Enabling a Greener Internet of Things. *Adv. Funct. Mater.* **2022**, *32*, 2200694. [CrossRef]
41. Reb, L.K.; Böhmer, M.; Predeschly, B.; Grott, S.; Weindl, C.L.; Ivandekic, G.I.; Guo, R.; Dreißigacker, C.; Gernhäuser, R.; Meyer, A.; et al. Perovskite and Organic Solar Cells on a Rocket Flight. *Joule* **2020**, *4*, 1880–1892. [CrossRef]
42. Cho, S.; Jung, D.; Kim, J.; Seo, J.; Ju, H.; Lee, J. Ultrathin GaAs Photovoltaic Arrays Integrated on a 1.4 mm Polymer Substrate for High Flexibility, a Lightweight Design, and High Specific Power. *Adv. Mater. Technol.* **2022**, *7*, 2200344. [CrossRef]
43. Schubert, M.B.; Werner, J.H. Flexible Solar Cells for Clothing. *Mater. Today* **2006**, *9*, 42–50. [CrossRef]
44. Li, X.; Li, P.; Wu, Z.; Luo, D.; Yu, H.-Y.; Lu, Z.-H. Review and Perspective of Materials for Flexible Solar Cells. *Mater. Rep. Energy* **2021**, *1*, 100001. [CrossRef]
45. Aslam, A.; Mehmood, U.; Arshad, M.H.; Ishfaq, A.; Zaheer, J.; Ul Haq Khan, A.; Sufyan, M. Dye-Sensitized Solar Cells (DSSCs) as a Potential Photovoltaic Technology for the Self-Powered Internet of Things (IoTs) Applications. *Sol. Energy* **2020**, *207*, 874–892. [CrossRef]
46. Michaels, H.; Rinderle, M.; Freitag, R.; Benesperi, I.; Edvinsson, T.; Socher, R.; Gagliardi, A.; Freitag, M. Dye-Sensitized Solar Cells under Ambient Light Powering Machine Learning: Towards Autonomous Smart Sensors for the Internet of Things. *Chem. Sci.* **2020**, *11*, 2895–2906. [CrossRef] [PubMed]
47. Mainville, M.; Leclerc, M. Recent Progress on Indoor Organic Photovoltaics: From Molecular Design to Production Scale. *ACS Energy Lett.* **2020**, *5*, 1186–1197. [CrossRef]
48. Cui, Y.; Hong, L.; Hou, J. Organic Photovoltaic Cells for Indoor Applications: Opportunities and Challenges. *ACS Appl. Mater. Interfaces* **2020**, *12*, 38815–38828. [CrossRef] [PubMed]
49. Jahandar, M.; Kim, S.; Lim, D.C. Indoor Organic Photovoltaics for Self-Sustaining IoT Devices: Progress, Challenges and Practicalization. *ChemSusChem* **2021**, *14*, 3449–3474. [CrossRef]

50. Mathews, I.; Kantareddy, S.N.R.; Sun, S.; Layurova, M.; Thapa, J.; Correa-Baena, J.-P.; Bhattacharyya, R.; Buonassisi, T.; Sarma, S.; Peters, I.M. Self-Powered Sensors Enabled by Wide-Bandgap Perovskite Indoor Photovoltaic Cells. *Adv. Funct. Mater.* **2019**, *29*, 1904072. [CrossRef]
51. Polyzoidis, C.; Rogdakis, K.; Kymakis, E. Indoor Perovskite Photovoltaics for the Internet of Things—Challenges and Opportunities toward Market Uptake. *Adv. Energy Mater.* **2021**, *11*, 2101854. [CrossRef]
52. Olzhabay, Y.; Ng, A.; Ukaegbu, I.A. Perovskite PV Energy Harvesting System for Uninterrupted IoT Device Applications. *Energies* **2021**, *14*, 7946. [CrossRef]
53. Thomas, S.K.; Pockett, A.; Seunarine, K.; Spence, M.; Raptis, D.; Meroni, S.; Watson, T.; Jones, M.; Carnie, M.J. Will the Internet of Things Be Perovskite Powered? Energy Yield Measurement and Real-World Performance of Perovskite Solar Cells in Ambient Light Conditions. *IoT* **2022**, *3*, 109–121. [CrossRef]
54. Tartagni, M.; Belleville, M.; Cantatore, E.; Fanet, H. *Energy Autonomous Systems: Future Trends in Devices, Technology, and Systems*; CATRENE: Paris, France, 2009; ISBN 978-88-904399-0-2.
55. Mumtaz, S.; Jornet, J.M.; Aulin, J.; Gerstacker, W.H.; Dong, X.; Ai, B. Terahertz Communication for Vehicular Networks. *IEEE Trans. Veh. Technol.* **2017**, *66*, 5617–5625. [CrossRef]
56. Ziar, H.; Manganiello, P.; Isabella, O.; Zeman, M. Photovoltatronics: Intelligent PV-Based Devices for Energy and Information Applications. *Energy Environ. Sci.* **2021**, *14*, 106–126. [CrossRef]
57. Chowdhury, M.Z.; Shahjalal, M.; Ahmed, S.; Jang, Y.M. 6G Wireless Communication Systems: Applications, Requirements, Technologies, Challenges, and Research Directions. *IEEE Open J. Commun. Soc.* **2020**, *1*, 957–975. [CrossRef]
58. Jungnickel, V.; Hinrichs, M.; Bober, K.L.; Kottke, C.; Corici, A.A.; Emmelmann, M.; Rufo, J.; Bök, P.; Behnke, D.; Riege, M.; et al. Enhance Lighting for the Internet of Things. In Proceedings of the 2019 Global LIFI Congress (GLC), Paris, France, 12–13 June 2019; pp. 1–6.
59. Hamza, A.; Tripp, T. Optical Wireless Communication for the Internet of Things: Advances, Challenges, and Opportunities. *TechRxiv* **2020**. [CrossRef]
60. Ghassemlooy, Z.; Alves, L.N.; Zvanovec, S.; Khalighi, M.-A. *Visible Light Communications: Theory and Applications*; CRC Press: Boca Raton, FL, USA, 2017; ISBN 978-1-4987-6754-5.
61. Kim, S.; Won, J.; Nahm, S. Simultaneous Reception of Solar Power and Visible Light Communication Using a Solar Cell. *Opt. Eng.* **2014**, *53*, 046103. [CrossRef]
62. Wang, Z.; Tsonev, D.; Videv, S.; Haas, H. Towards Self-Powered Solar Panel Receiver for Optical Wireless Communication. In Proceedings of the 2014 IEEE International Conference on Communications (ICC), Sydney, Australia, 10–14 June 2014; pp. 3348–3353.
63. Wang, Z.; Tsonev, D.; Videv, S.; Haas, H. On the Design of a Solar-Panel Receiver for Optical Wireless Communications With Simultaneous Energy Harvesting. *IEEE J. Sel. Areas Commun.* **2015**, *33*, 1612–1623. [CrossRef]
64. Lee, S.H. A Passive Transponder for Visible Light Identification Using a Solar Cell. *IEEE Sens. J.* **2015**, *15*, 5398–5403. [CrossRef]
65. Pathak, P.H.; Feng, X.; Hu, P.; Mohapatra, P. Visible Light Communication, Networking, and Sensing: A Survey, Potential and Challenges. *IEEE Commun. Surv. Tutor.* **2015**, *17*, 2047–2077. [CrossRef]
66. Bishnu, A.; Das, S.K.; Soni, M.; Bhatia, V. Comparative Analysis of Low Cost Photodetectors for Visible Light Communication. In Proceedings of the International Symposium on Advanced Networks and Telecommunication Systems, ANTS, Indore, India, 16–19 December 2018. [CrossRef]
67. Diamantoulakis, P.D.; Karagiannidis, G.K.; Ding, Z. Simultaneous Lightwave Information and Power Transfer (SLIPT). *IEEE Trans. Green Commun. Netw.* **2018**, *2*, 764–773. [CrossRef]
68. Ma, S.; Zhang, F.; Li, H.; Zhou, F.; Wang, Y.; Li, S. Simultaneous Lightwave Information and Power Transfer in Visible Light Communication Systems. *IEEE Trans. Wirel. Commun.* **2019**, *18*, 5818–5830. [CrossRef]
69. Pan, G.; Diamantoulakis, P.D.; Ma, Z.; Ding, Z.; Karagiannidis, G.K. Simultaneous Lightwave Information and Power Transfer: Policies, Techniques, and Future Directions. *IEEE Access* **2019**, *7*, 28250–28257. [CrossRef]
70. Uysal, M.; Ghasvarianjahromi, S.; Karbalayghareh, M.; Diamantoulakis, P.D.; Karagiannidis, G.K.; Sait, S.M. SLIPT for Underwater Visible Light Communications: Performance Analysis and Optimization. *IEEE Trans. Wirel. Commun.* **2021**, *20*, 6715–6728. [CrossRef]
71. Filho, J.I.D.O.; Alkhazragi, O.; Trichili, A.; Ooi, B.S.; Alouini, M.-S.; Salama, K.N. Simultaneous Lightwave and Power Transfer for Internet of Things Devices. *Energies* **2022**, *15*, 2814. [CrossRef]
72. Alamu, O.; Olwal, T.O.; Djouani, K. Simultaneous Lightwave Information and Power Transfer in Optical Wireless Communication Networks: An Overview and Outlook. *Optik* **2022**, *266*, 169590. [CrossRef]
73. Sarwar, R.; Sun, B.; Kong, M.; Ali, T.; Yu, C.; Cong, B.; Xu, J. Visible Light Communication Using a Solar-Panel Receiver. In Proceedings of the 2017 16th International Conference on Optical Communications and Networks (ICOCN), Wuzhen, China, 7–10 August 2017; pp. 1–3.
74. Malik, B.; Zhang, X. Solar Panel Receiver System Implementation for Visible Light Communication. In Proceedings of the 2015 IEEE International Conference on Electronics, Circuits, and Systems (ICECS), Cairo, Egypt, 6–9 December 2015; pp. 502–503.
75. Shin, W.-H.; Yang, S.-H.; Kwon, D.-H.; Han, S.-K. Self-Reverse-Biased Solar Panel Optical Receiver for Simultaneous Visible Light Communication and Energy Harvesting. *Opt. Exp.* **2016**, *24*, A1300–A1305. [CrossRef] [PubMed]

76. Kadirvelu, S.; Leon-Salas, W.D.; Fan, X.; Kim, J.; Peleato, B.; Mohammadi, S.; Vijayalakshmi, B. A Circuit for Simultaneous Reception of Data and Power Using a Solar Cell. *IEEE Trans. Green Commun. Netw.* **2021**, *5*, 2065–2075. [CrossRef]
77. Wu, J.-T.; Chow, C.-W.; Liu, Y.; Hsu, C.-W.; Yeh, C.-H. Performance Enhancement Technique of Visible Light Communications Using Passive Photovoltaic Cell. *Opt. Commun.* **2017**, *392*, 119–122. [CrossRef]
78. Wang, H.-Y.; Wu, J.-T.; Chow, C.-W.; Liu, Y.; Yeh, C.-H.; Liao, X.-L.; Lin, K.-H.; Wu, W.-L.; Chen, Y.-Y. Using Pre-Distorted PAM-4 Signal and Parallel Resistance Circuit to Enhance the Passive Solar Cell Based Visible Light Communication. *Opt. Commun.* **2018**, *407*, 245–249. [CrossRef]
79. Das, S.; Fakidis, J.; Sparks, A.; Poves, E.; Videv, S.; Haas, H. Towards 100 Mb/s Optical Wireless Communications Using a Silicon Photovoltaic Receiver. In Proceedings of the GLOBECOM 2020—2020 IEEE Global Communications Conference, Taipei, Taiwan, 7–11 December 2020; pp. 1–6.
80. Bialic, E.; Maret, L.; Kténas, D. Specific Innovative Semi-Transparent Solar Cell for Indoor and Outdoor LiFi Applications. *Appl. Opt.* **2015**, *54*, 8062–8069. [CrossRef]
81. Lorrière, N.; Bialic, E.; Pasquinelli, M.; Chabriel, G.; Barrère, J.; Escoubas, L.; Simon, J. An OFDM Testbed for LiFi Performance Characterization of Photovoltaic Modules. In Proceedings of the 2018 Global LIFI Congress (GLC), Paris, France, 8–9 February 2018; pp. 1–5.
82. Sindhubala, K.; Vijayalakshmi, B. Receiver Intend to Reduce Ambient Light Noise in Visible-Light Communication Using Solar Panels. *J. Eng. Sci. Technol. Rev.* **2017**, *10*, 84–90. [CrossRef]
83. Fakidis, J.; Videv, S.; Helmers, H.; Haas, H. 0.5-Gb/s OFDM-Based Laser Data and Power Transfer Using a GaAs Photovoltaic Cell. *IEEE Photonics Technol. Lett.* **2018**, *30*, 841–844. [CrossRef]
84. Fakidis, J.; Helmers, H.; Haas, H. Simultaneous Wireless Data and Power Transfer for a 1-Gb/s GaAs VCSEL and Photovoltaic Link. *IEEE Photonics Technol. Lett.* **2020**, *32*, 1277–1280. [CrossRef]
85. Kong, M.; Lin, J.; Kang, C.H.; Shen, C.; Guo, Y.; Sun, X.; Sait, M.; Weng, Y.; Zhang, H.; Ng, T.K.; et al. Toward Self-Powered and Reliable Visible Light Communication Using Amorphous Silicon Thin-Film Solar Cells. *Opt. Exp.* **2019**, *27*, 34542. [CrossRef] [PubMed]
86. Majlesein, B.; Guerra, V.; Rabadan, J.; Rufo, J.; Perez-Jimenez, R. Evaluation of Communication Link Performance and Charging Speed in Self-Powered Internet of Underwater Things Devices. *IEEE Access* **2022**, *10*, 100566–100575. [CrossRef]
87. Lei, W.; Chen, Z.; Xu, Y.; Jiang, C.; Lin, J.; Fang, J. Negatively Biased Solar Cell Optical Receiver for Underwater Wireless Optical Communication System With Low Peak Average Power Ratio. *IEEE Photonics J.* **2022**, *14*, 3186702. [CrossRef]
88. Liu, Y.; Chen, H.-Y.; Liang, K.; Hsu, C.-W.; Chow, C.-W.; Yeh, C.-H. Visible Light Communication Using Receivers of Camera Image Sensor and Solar Cell. *IEEE Photonics J.* **2016**, *8*, 2507364. [CrossRef]
89. Hsu, C.-W.; Wu, J.-T.; Wang, H.-Y.; Chow, C.-W.; Lee, C.-H.; Chu, M.-T.; Yeh, C.-H. Visible Light Positioning and Lighting Based on Identity Positioning and RF Carrier Allocation Technique Using a Solar Cell Receiver. *IEEE Photonics J.* **2016**, *8*, 2590945. [CrossRef]
90. Carrascal, C.; Demirkol, I.; Paradells, J. On-Demand Sensor Node Wake-up Using Solar Panels and Visible Light Communication. *Sensors* **2016**, *16*, 418. [CrossRef]
91. Das, S.; Poves, E.; Fakidis, J.; Sparks, A.; Videv, S.; Haas, H. Towards Energy Neutral Wireless Communications: Photovoltaic Cells to Connect Remote Areas. *Energies* **2019**, *12*, 3772. [CrossRef]
92. Hegedus, S. *Handbook of Photovoltaic Science and Engineering*; Wiley Online Library: Hoboken, NJ, USA, 2003; ISBN 0-471-49196-9.
93. Lorrière, N.; Bétrancourt, N.; Pasquinelli, M.; Chabriel, G.; Barrère, J.; Escoubas, L.; Wu, J.-L.; Bermudez, V.; Ruiz, C.M.; Simon, J.-J. Photovoltaic Solar Cells for Outdoor LiFi Communications. *J. Lightwave Technol.* **2020**, *38*, 3822–3831. [CrossRef]
94. Sepehrvand, S.; Theagarajan, L.N.; Hranilovic, S. Rate-Power Trade-Off in Simultaneous Lightwave Information and Power Transfer Systems. *IEEE Commun. Lett.* **2021**, *25*, 1249–1253. [CrossRef]
95. Chen, S.; Liu, L.; Chen, L.-K. On the Nonlinear Distortion Characterization in Photovoltaic Modules for Visible Light Communication. *IEEE Photonics Technol. Lett.* **2021**, *33*, 1467–1470. [CrossRef]
96. Das, S.; Sparks, A.; Poves, E.; Videv, S.; Fakidis, J.; Haas, H. Effect of Sunlight on Photovoltaics as Optical Wireless Communication Receivers. *J. Lightwave Technol.* **2021**, *39*, 6182–6190. [CrossRef]
97. Arredondo, B.; Romero, B.; Pena, J.M.S.; Fernández-Pacheco, A.; Alonso, E.; Vergaz, R.; De Dios, C. Visible Light Communication System Using an Organic Bulk Heterojunction Photodetector. *Sensors* **2013**, *13*, 12266–12276. [CrossRef]
98. Vega-Colado, C.; Arredondo, B.; Torres, J.C.; López-Fraguas, E.; Vergaz, R.; Martín-Martín, D.; Del Pozo, G.; Romero, B.; Apilo, P.; Quintana, X.; et al. An All-Organic Flexible Visible Light Communication System. *Sensors* **2018**, *18*, 3045. [CrossRef]
99. López-Fraguas, E.; Arredondo, B.; Vega-Colado, C.; del Pozo, G.; Najafi, M.; Martín-Martín, D.; Galagan, Y.; Sánchez-Pena, J.M.; Vergaz, R.; Romero, B. Visible Light Communication System Using an Organic Emitter and a Perovskite Photodetector. *Org. Electron.* **2019**, *73*, 292–298. [CrossRef]
100. Zhang, S.; Tsonev, D.; Videv, S.; Ghosh, S.; Turnbull, G.A.; Samuel, I.D.W.; Haas, H. Organic Solar Cells as High-Speed Data Detectors for Visible Light Communication. *Optica* **2015**, *2*, 607. [CrossRef]
101. Liang, Y.; Xu, Z.; Xia, J.; Tsai, S.-T.; Wu, Y.; Li, G.; Ray, C.; Yu, L.; Yu, L.P.; Liang, Y.Y.; et al. For the Bright Future—Bulk Heterojunction Polymer Solar Cells with Power Conversion Efficiency of 7.4%. *Adv. Mater.* **2010**, *22*, E135–E138. [CrossRef]
102. He, Z.; Zhong, C.; Huang, X.; Wong, W.Y.; Wu, H.; Chen, L.; Su, S.; Cao, Y. Simultaneous Enhancement of Open-Circuit Voltage, Short-Circuit Current Density, and Fill Factor in Polymer Solar Cells. *Adv. Mater.* **2011**, *23*, 4636–4643. [CrossRef] [PubMed]

103. Heremans, P.; Tripathi, A.K.; de Jamblinne de Meux, A.; Smits, E.C.P.; Hou, B.; Pourtois, G.; Gelinck, G.H. Mechanical and Electronic Properties of Thin-Film Transistors on Plastic, and Their Integration in Flexible Electronic Applications. *Adv. Mater.* **2016**, *28*, 4266–4282. [CrossRef] [PubMed]
104. ASCA® | The Photovoltaic Solution That Unlocks Your Imagination. Available online: https://www.asca.com/ (accessed on 22 November 2022).
105. Lorriere, N.; Chabriel, G.; Barrere, J.; Pasquinelli, M.; Pic, G.; Vannieuwenhuyse, N.; Escoubas, L.; Simon, J.-J. LiFi Reception from Organic Photovoltaic Modules Subject to Additional DC Illuminations and Shading Effects. In Proceedings of the 2019 Global LIFI Congress (GLC), Paris, France, 12–13 June 2019; IEEE: Manhattan, NY, USA, 2019; pp. 1–5.
106. Hofer, J.; Groenewolt, A.; Jayathissa, P.; Nagy, Z.; Schlueter, A. Parametric Analysis and Systems Design of Dynamic Photovoltaic Shading Modules. *Energy Sci. Eng.* **2016**, *4*, 134–152. [CrossRef]
107. Mica, N.A.; Bian, R.; Manousiadis, P.; Jagadamma, L.K.; Tavakkolnia, I.; Haas, H.; Turnbull, G.A.; Samuel, I.D.W. Triple-Cation Perovskite Solar Cells for Visible Light Communications. *Photonics Res.* **2020**, *8*, A16. [CrossRef]
108. Saliba, M.; Matsui, T.; Seo, J.-Y.; Domanski, K.; Correa-Baena, J.-P.; Nazeeruddin, M.K.; Zakeeruddin, S.M.; Tress, W.; Abate, A.; Hagfeldt, A.; et al. Cesium-Containing Triple Cation Perovskite Solar Cells: Improved Stability, Reproducibility and High Efficiency. *Energy Environ. Sci.* **2016**, *9*, 1989–1997. [CrossRef] [PubMed]
109. Tavakkolnia, I.; Jagadamma, L.K.; Bian, R.; Manousiadis, P.P.; Videv, S.; Turnbull, G.A.; Samuel, I.D.W.; Haas, H. Organic Photovoltaics for Simultaneous Energy Harvesting and High-Speed MIMO Optical Wireless Communications. *Light Sci. Appl.* **2021**, *10*, 41. [CrossRef] [PubMed]
110. Wang, K.; Liu, C.; Meng, T.; Yi, C.; Gong, X. Inverted Organic Photovoltaic Cells. *Chem. Soc. Rev.* **2016**, *45*, 2937–2975. [CrossRef]
111. Zhang, J.; Tan, H.S.; Guo, X.; Facchetti, A.; Yan, H. Material Insights and Challenges for Non-Fullerene Organic Solar Cells Based on Small Molecular Acceptors. *Nat. Energy* **2018**, *3*, 720–731. [CrossRef]
112. Li, P.; Lu, Z.-H. Interface Engineering in Organic Electronics: Energy-Level Alignment and Charge Transport. *Small Sci.* **2021**, *1*, 2000015. [CrossRef]
113. Li, Y.; Xie, H.; Lim, E.L.; Hagfeldt, A.; Bi, D. Recent Progress of Critical Interface Engineering for Highly Efficient and Stable Perovskite Solar Cells. *Adv. Energy Mater.* **2022**, *12*, 2102730. [CrossRef]
114. Hawashin, H.; Karthick, S.; Ratier, B.; Trigaud, T.; Bouclé, J. Perovskite solar cells as energy harvesters and data receivers for visible light communications (VLC). In Proceedings of the 6ème e-Journées Pérovskites Halogénées, Palaiseau, France, 31 March–2 April 2021.
115. Hawashin, H.; Moline, B.; Julien-Vergonjanne, A.; Sahuguede, S.; Antony, R.; Trigaud, T.; Bouclé, J. Application of Inverted Organic Solar Cells for Energy Harvesting and Visible Light Communications (VLC). In Proceedings of the 6ème Colloque Francophone PLUridisciplinaire sur les Matériaux, l'Environnement et l'Electronique, Limoges, France, 10–12 April 2019.
116. Nelson, J. *The Physics of Solar Cells*; Imperial College Press: London, UK, 2003; ISBN 978-1-86094-349-2.
117. Weddell, A.S.; Merrett, G.V.; Al-Hashimi, B.M. Ultra Low-Power Photovoltaic MPPT Technique for Indoor and Outdoor Wireless Sensor Nodes. In Proceedings of the Design, Automation and Test in Europe, Grenoble, France, 14–18 March 2011; pp. 905–908. [CrossRef]